WOODS HOLE OCEANOGRAPHIC INSTITUTION

Woods Hole, Massachusetts

Reference No. 53-30

MARINE METEOROLOGY

Some Results of a Trade Cumulus Cloud Investigation

By

Joanne Starr Malkus

Technical Report No. 23
Submitted to the Office of Naval Research
Under Contract N6onr-27702 (NR-082-021)

May 1953

APPROVED FOR DISTRIBUTION [signature]
Director

TABLE OF CONTENTS

SOME RESULTS OF A TRADE CUMULUS CLOUD INVESTIGATION

By

Joanne Starr Malkus

Abstract

Cross sections through two trade cumulus clouds are presented, showing the temperatures, turbulence, and water vapor content of the clouds and their nearby environment, the cloud slope, and the external wind profile. The two clouds were studied over the Caribbean Sea on the same afternoon in June, 1952, and were in widely differing phases of their life cycles. The measurements were made from a slow-flying aircraft equipped with sensing instruments and whose behavior as a meteorological tool had been previously studied. Numerous calculations are made from the cross sections, including total and dynamic entrainment, drafts, slopes, and liquid water content. These are, where possible, checked against the corresponding observations. In addition to testing previously evolved theoretical models, and the usefulness of the steady-state hypothesis, the data provide some evidence concerning the formation and growth of larger trade cumulus clouds from several smaller ones and by successive stages.

I INTRODUCTION

The important role of trade cumulus clouds in the budgets of the low-latitude atmosphere and in the energy supply for the global wind systems has been established. These marine clouds are, furthermore, examples of the convective process operating under more uniform and relatively less complex conditions than in the case of land cumulus in middle latitudes. Finally, trade cumuli are the major cloud forms which commonly produce precipitation at above freezing temperatures. Although the present study is not directly concerned with condensation and precipitation processes, it is contended that without the introduction of information concerning the draft structure and dynamics of the clouds, the growth of theories in the field of "cloud physics" and precipitation must be drastically hampered.

Important advances in trade cumulus dynamics began with the Wyman-Woodcock Caribbean Expedition in 1946. Their results revealed several important features of these clouds, among them 1) the cumuli appeared not to possess "roots", or cloud-scale drafts extending well below individual cloud bases and 2) a significant amount of mixing (entrainment) between cloud and environment was inferred from comparison between cloud and clear air temperature and moisture soundings (Stommel, 1947).

Since this time considerable work has been done on a steady-state model of trade cumulus, based on ideas of entrainment. Relative horizontal cloud-air motions have been studied, and the dependence of cumulus slopes on cloud and environment

parameters have been predicted. So far, a time-dependent, or life cycle, cumulus model has not been evolved. Prior to such an attempt, it has been considered necessary to answer certain questions by further observations. In addition to the checking of the Wyman-Woodcock results and the foregoing cited theoretical work, it was necessary to investigate carefully the resistance forces operating against cumulus growth. It was desired to determine whether a functional dependence of entrainment upon cloud and environment parameters would be established, and whether or not additional resistances due to "form drag" or pressure forces must be taken into account.

To answer these questions, nearly simultaneous cross sections at several levels through a cloud and nearby environment were desired. These should include measurement of drafts, turbulence, temperature, water vapor and liquid water content, cloud slope and environment wind shear. To obtain such observations, a PBY-6A aircraft was secured by the Woods Hole Oceanographic Institution, on loan through the Office of Naval Research and the Bureau of Aeronautics, U. S. Navy. The extensive studies of this airplane as a meteorological tool and the details of its instrumentation will be discussed in other reports by this group. The present paper is confined largely to a discussion of some of the results of measurement and the calculations therefrom. The consistency of these, or lack thereof, will provide an indication of the adequacy of the instrumentation.

II METHODS OF MEASUREMENT AND OBSERVATIONAL PROCEDURES

The clouds were investigated by the airplane in the manner shown in Figure 1. Prior to entering the selected cloud at the topmost level, the aircraft passed the tower (flying downwind) at a distance of several miles to obtain one or two still photographs of its slope in the plane of the wind. The cloud was always first entered at the same altitude at which the photograph was taken. This information, in addition to knowledge of the height of cloud base, permitted accurate reconstruction of the cross section by combinations of the airplane records and the photographs. The airplane was ordinarily flown at an airspeed of about 50-60 meters/sec. The cross section of a single cloud, consisting of five to seven horizontal runs, could be completed in a time interval of 15-25 minutes. Prior to the field work, it was doubted whether any cloud would remain in even a quasi-steady state for this length of time, and therefore whether calculations based upon the steady-state models would be meaningful. The present paper should indicate where and to what degree these doubts are justified.

During June 1952 field work in the vicinity of San Juan, Puerto Rico, several clouds were examined in which all the desired measurements, except that of liquid water, were obtained to varying degress of accuracy. The temperatures and water vapor contents were obtained from records by a modified form of the M.I.T. psychrograph, the performance and accuracy of which are discussed elsewhere (McCasland, 1951). It is pertinent to note that since

CLOUD PROCEDURE

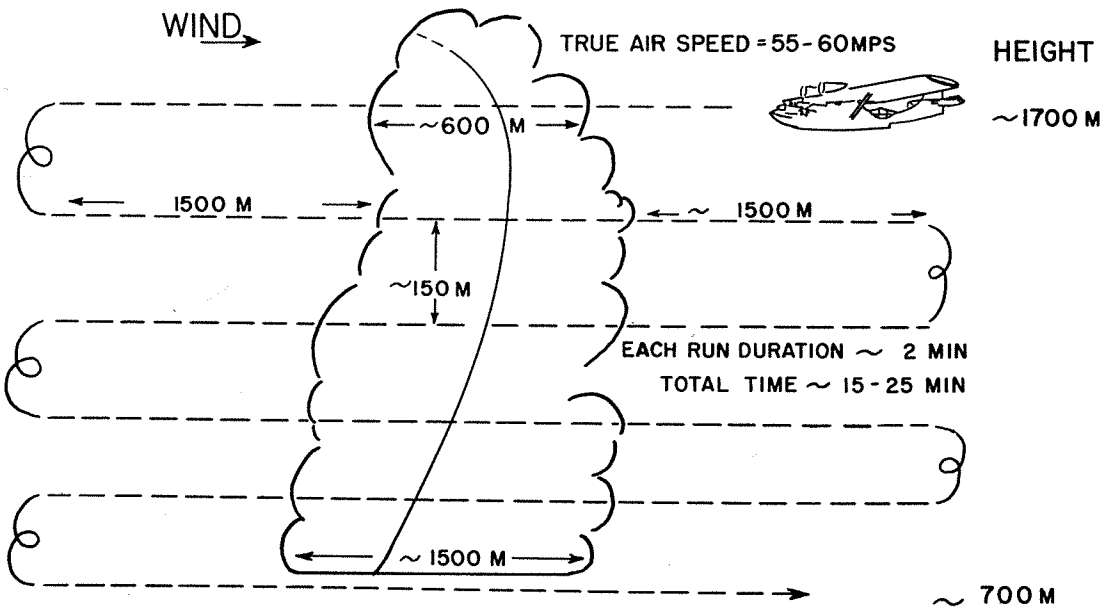

FIG. 1

the response time of this instrument is approximately two seconds, the records of dry- and wet-bulb temperatures, virtual temperatures and mixing ratio represent averages over roughly 100 m horizontal distance. The turbulence is described by a parameter called "turbulence index" introduced earlier by Malkus and Bunker (1952). It is determined from the records of a water column accelerometer.[1] External wind profiles were obtained by double drift of the aircraft and although drifts were determined independently by two sights and observers, these results are probably less accurate than single theodolite pilot balloon observations, especially when whitecaps were absent from the sea surface. (Use smoke flares)

The most crucial measurements were of ~~drafts~~ vertical motions. These were obtained by integration of the records of the water column accelerometer. Studies of the flight characteristics of the aircraft leading to justification of this method are reported on by Brewer (1953). It was attempted to fly the airplane at constant attitude and airspeed in the cloud runs, and if this assumption were exact, the vertical motions of the air are given by the following equation:

$$w = \sum \bar{a} \Delta t + \frac{1.25\ \bar{a}\ M}{\frac{1}{2}\rho S V (dC_L/d\alpha)} \qquad (1)$$

---

[1] "Accelerometer for air turbulence measurements" by Allyn C. Vine. Memorandum on file at the Woods Hole Oceanographic Institution, August 1945.

where $\bar{a}$ is the average observed vertical acceleration of the airplane during Δt, M is its mass, ρ the air density, S the wing area, V the airspeed, and $dC_L/d\alpha$ the variation in lift coefficient with angle of attack, known for this airplane. The first term to the right of the equality sign gives the vertical velocity of the aircraft relative to the ground, while the second term gives the sinking speed of the plane through the air. This equation, its derivation and use are discussed in more detail by Bunker (1953).

Recent modification of the PBY instrumentation will permit corrections for deviations from constant airspeed and attitude, not feasible on the 1952 field work. Under optimum flying by the pilot, errors due to fluctuations in these quantities may amount to $\pm$ 50 cm/sec in a single measurement, the larger contribution usually arising from attitude departures. The space-averaged draft records presented here can be relied on to somewhat better than this amount. During the 1952 program, a large number of clouds were penetrated. In only a very small fraction of these did it prove possible to fly with sufficiently small attitude variations to make feasible the application of equation (1).

Two such clouds were encountered on June 28, 1952, near St. Croix, Virgin Islands. On this day all instruments were working well, and fairly isolated clouds persisted under apparently steady conditions during seven or more horizontal passes by the airplane. The two clouds studied possessed upper portions or towers in widely differing phases of their life cycles. The one being in the very active phase, perhaps still growing, in which

no significant downdrafts were present; the other tower, although not apparently evaporating, was in a more mature phase with strong downdrafts present near its top. This and other aspects of the two clouds form a very interesting contrast.

III THE CALCULATIONS TO BE MADE

Before presenting the data for these two clouds, it will be well to outline the calculations in terms of which the questions have been framed. Most of these concern the resistive influences upon the drafts.

First, based on the method of Stommel (1947), it is possible to calculate the total amount of outside air mixed with the draft from one level to the next, called "gross entrainment" by Malkus (1952a). This is done from the psychrograph records by a comparison of temperatures and moisture contents of drafts and nearby environment. Second, by a modification of Stommel's method (Stommel, 1951) it is possible to calculate the draft velocity profile from the observed virtual temperatures and draft diameters as a function of height. This is now possible without any assumption concerning what fraction of the entrained air is retained within the draft. The results may be compared with the observed draft profile and the velocity of the unmixed parcel.

The vertical equation of motion for a steady-state, homogeneous draft may be written

$$\frac{d}{dz}(Mw) = \alpha A \rho \qquad (2)$$

where M is the mass flux; w is the vertical velocity of the draft (assumed discontinuously distinct from the environment); α is the buoyancy force per unit mass and can be written $g\ T_v - T_v'/T_v'$ where T_v is the virtual temperature of the draft, T_v' is the virtual temperature of the environment and g is the acceleration of gravity. A is the cross-sectional area of the draft; ρ is its density, and the z axis is positive upwards.

Since

$$M = \rho A w \tag{3}$$

(2) can be written

$$\frac{d}{dz}(\rho A w^2) = \alpha A \rho = \rho A w^2 \left(\frac{1}{\rho}\frac{d\rho}{dz} + \frac{1}{A}\frac{dA}{dz} + \frac{2}{w}\frac{dw}{dz}\right) \tag{4}$$

The term $\frac{1}{\rho}\frac{d\rho}{dz}$ is several orders of magnitude less than the others beside it and may be neglected. Therefore,

$$\frac{\alpha}{w^2} = \frac{1}{A}\frac{dA}{dz} + \frac{2}{w}\frac{dw}{dz} \tag{5}$$

For the unmixed parcel, the equation of motion leads to

$$\frac{dw}{dz} = \frac{\alpha}{w} \tag{6}$$

For the calculations to follow, the integration of (5) is done stepwise from a lower level z_o to the next highest, z_1 , namely,

$$\frac{\bar{\alpha}}{w_o^2} = \frac{1}{\bar{A}} \frac{dA}{z_1 - z_o} + \frac{2}{w_o} \frac{\Delta w}{z_1 - z_o} \qquad (7)$$

where the bars indicate the mean of the observations at z_o and z_1 and the integration is started by taking the observed w_o at the lowest level of the cloud investigated.

It is then possible to calculate the amount of entrainment required to fulfill continuity (~~called "dynamic entrainment" by Houghton and Cramer, 1951~~), and to compare this with the gross entrainment found by Stommel's method. It will be important to note whether these independent results are consistent and whether and under what conditions the gross entrainment exceeds that required by continuity.

While a comparison of measured with calculated draft profiles should yield some idea of whether significant amounts of "form drag" are resisting the vertical growth of the cumuli, the cloud slope may be calculated to enquire about horizontal resistance forces. This method has been described in detail by Malkus (1952b). Its present application will consist in finding the relative cloud-air horizontal velocity on the basis of the observed wind shear and considering that the measured entrainment is the only horizontal resistance. The cloud slope computed on this hypothesis is then to be compared with that photographed. If the observed cloud slants more than the amount computed, it may be inferred that significant horizontal form drag is operative.

Finally, it was desired to investigate the structure of small-scale turbulence (eddies 50-150 m diameter) in and around

trade cumulus. It was especially desired to learn whether its strong development, indicated by high values of turbulence index, could be related to the presence of active updrafts. This has often been assumed to be the case, especially in those situations where drafts have not been measured and it has been sought to locate them roughly from accelerometer records which for various reasons could not be integrated reliably. Therefore, correlations between turbulence index and drafts have been undertaken for each run. Similar correlations between turbulence index and horizontal shear in vertical velocities have been made and the results will be presented in the discussion of each cloud which follows.

Although studied later in time and therefore called "Cloud II", the more active cloud will be discussed first as the data concerning it are more complete and the steady-state model calculations more satisfactory.

IV CLOUD II - JUNE 28, 1952

This cloud, photographed in the plane of the wind, is shown in Figure 2. It is seen to be a rather isolated cloud, larger than most of its neighbors, although not so large as one or two clouds seen at the same time which had reached cumulonimbus proportions. The airplane was able to make five traverses through the cloud and one just below its base in less than 25 minutes; and the cloud, when last seen nearly one hour after Figure 2 was made, was still vigorous and maintained the same general appearance. A summary of all the data obtained for this cloud is shown

in Figure 3. The original records were sidemarked in code to indicate entrance into and exit from the liquid cloud and it proved extremely easy to fit together the runs at various levels on the silhouette obtained from the photograph. It should be noted how this automatically led to excellent coincidence between the observed draft structure and the major features of the cloud as shown in the photograph. Strong drafts coincide with observed turrets and are consistently traceable from level to level.

Figures 4-9 give the individual runs at each height. It is interesting that the drafts appear to break up into "cells" as the 830 m level is reached. It is also interesting that from that level downward vertical holes through the base of the cloud were clearly visible. These features appeared common to nearly all the good-sized trade cumuli studied, and indicate that the larger clouds may have been formed from an aggregation of several small ones.

The results of the calculations cited in the foregoing section are next to be discussed.

a. Entrainment calculation

The calculation of gross entrainment by Stommel's method is given in Table I. It is important to point out that it is now possible to carry out this calculation specifically for the main draft in the cloud. This is significantly better than the earlier way, in which it was only possible to compare clear air to cloudy air.

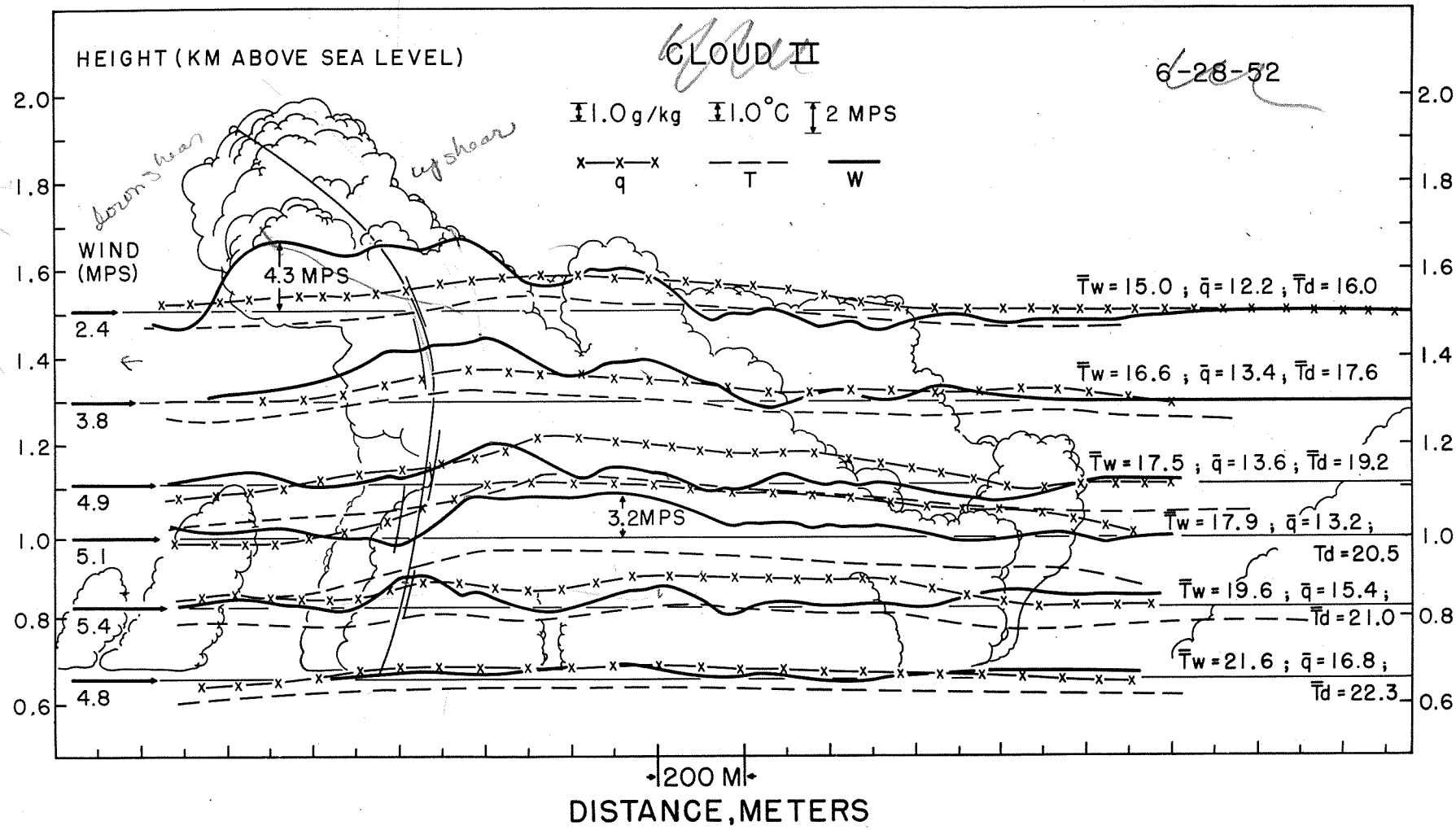
HEIGHT (KM ABOVE SEA LEVEL)
CLOUD II
6-28-52
1.0 g/kg
1.0°C
2 MPS
q
T
W
downshear
upshear
WIND (MPS)
4.3 MPS
3.2MPS
2.4
3.8
4.9
5.1
5.4
4.8
2.0
1.8
1.6
1.4
1.2
1.0
0.8
0.6
$\bar{T}w = 15.0$; $\bar{q} = 12.2$; $\bar{T}d = 16.0$
$\bar{T}w = 16.6$; $\bar{q} = 13.4$; $\bar{T}d = 17.6$
$\bar{T}w = 17.5$; $\bar{q} = 13.6$; $\bar{T}d = 19.2$
$\bar{T}w = 17.9$; $\bar{q} = 13.2$; $\bar{T}d = 20.5$
$\bar{T}w = 19.6$; $\bar{q} = 15.4$; $\bar{T}d = 21.0$
$\bar{T}w = 21.6$; $\bar{q} = 16.8$; $\bar{T}d = 22.3$
200 M
DISTANCE, METERS

FIG. 3

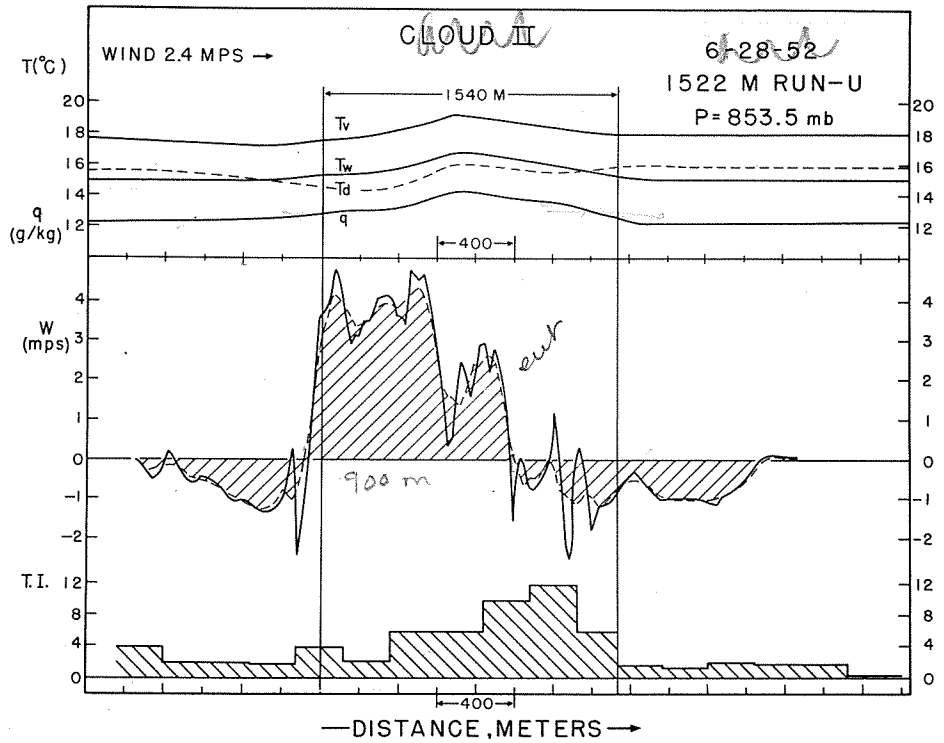
CLOUD III
WIND 2.4 MPS →
6-28-52
1522 M RUN-U
P = 853.5 mb
1540 M
T(°C)
Tv
Tw
Td
q
q (g/kg)
400
W (mps)
900 m
T.I.
400
—DISTANCE, METERS→

FIG. 4

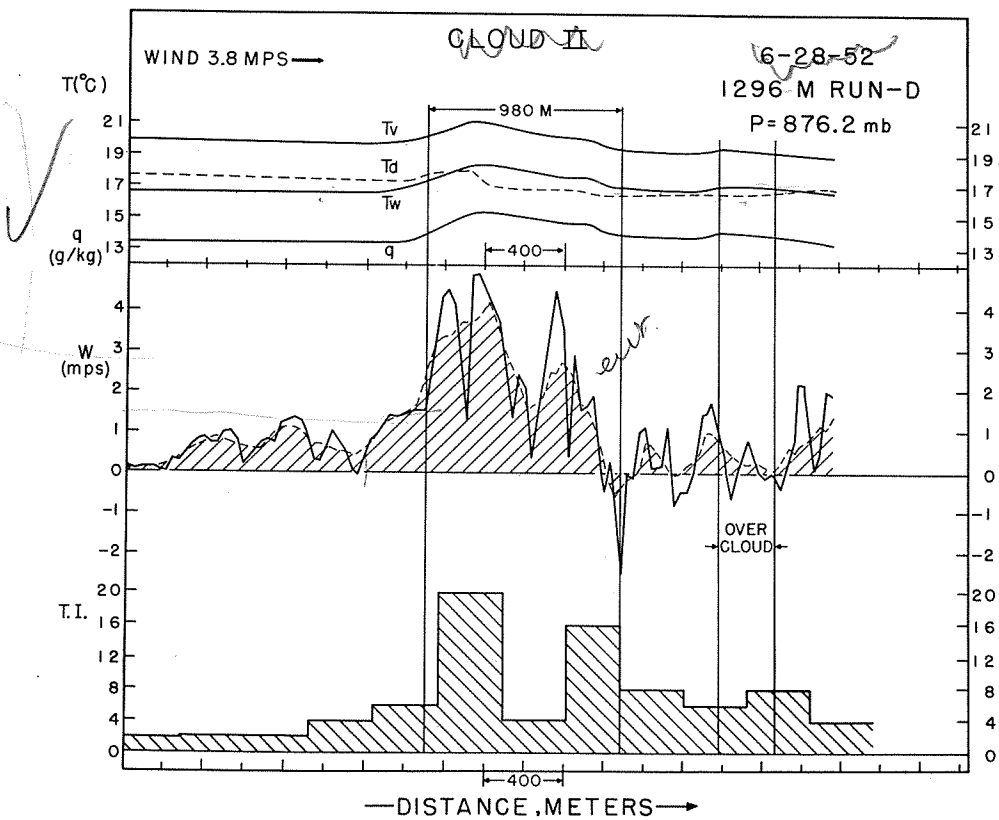
CLOUD II
WIND 3.8 MPS →
6-28-52
1296 M RUN-D
P = 876.2 mb
980 M
T(°C)
Tv
Td
Tw
q
q (g/kg)
400
W (mps)
OVER CLOUD
T.I.
400
—DISTANCE, METERS→

FIG. 5

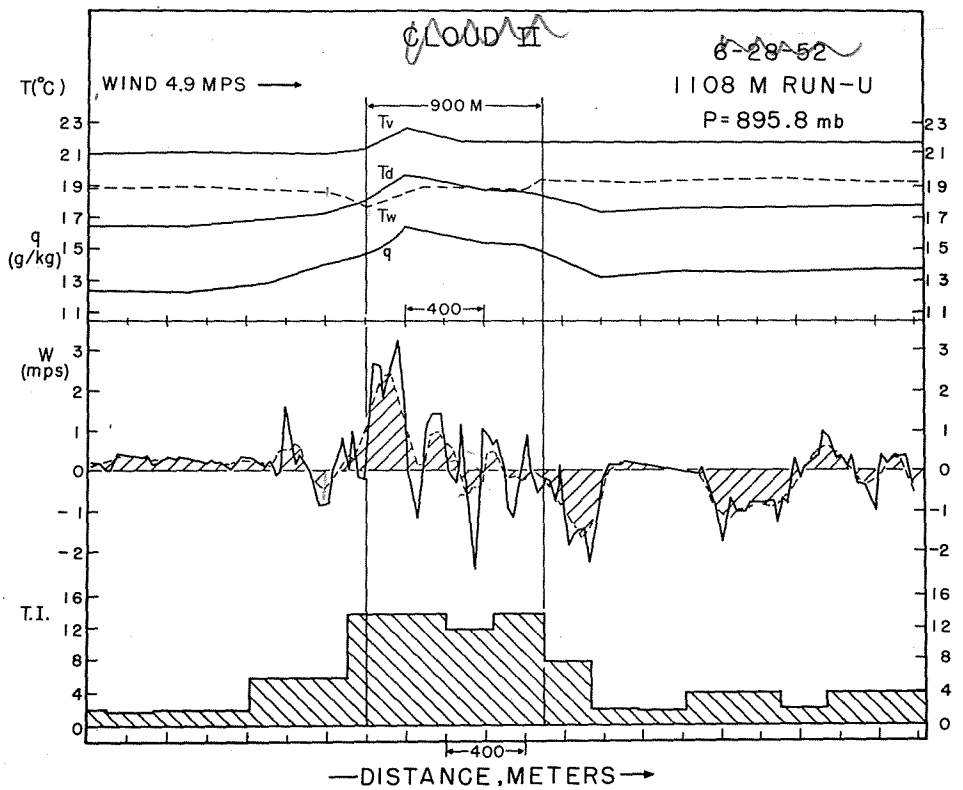
CLOUD II
6-28-52
T(°C)
WIND 4.9 MPS
900 M
1108 M RUN-U
P=895.8 mb
Tv
Td
Tw
q
q (g/kg)
400
W (mps)
T.I.
400
—DISTANCE, METERS—

FIG. 6

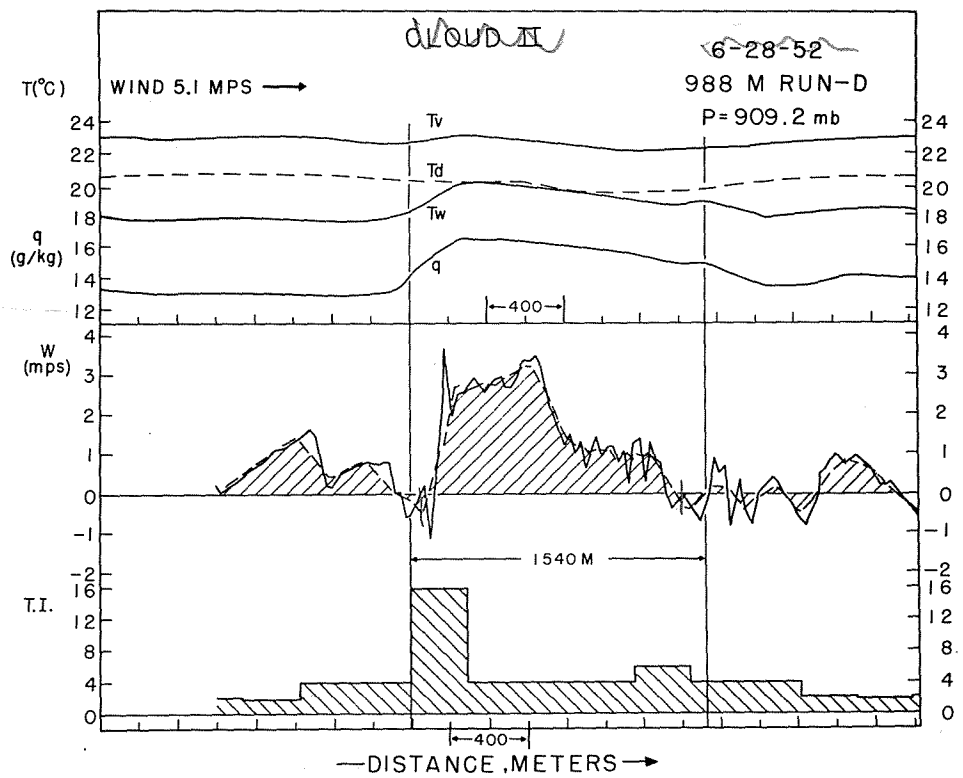
CLOUD II
6-28-52
T(°C)
WIND 5.1 MPS
988 M RUN-D
P=909.2 mb
Tv
Td
Tw
q
q (g/kg)
400
W (mps)
1540 M
T.I.
400
—DISTANCE, METERS—

FIG. 7

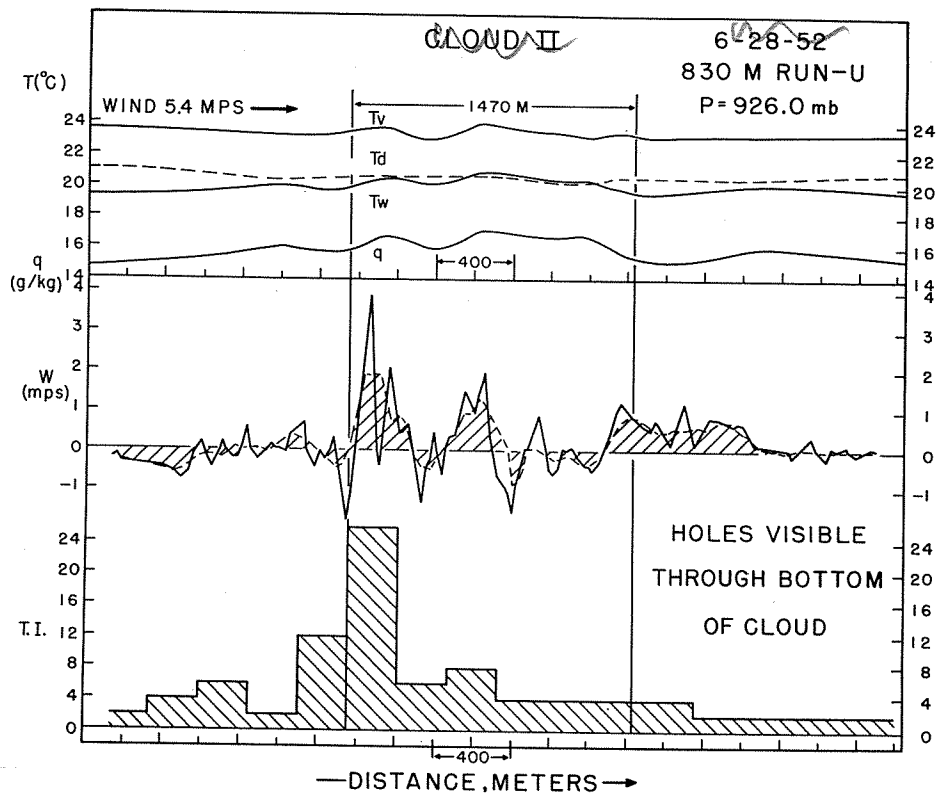
CLOUD II
6-28-52
830 M RUN-U
P=926.0 mb
WIND 5.4 MPS
1470 M
T(°C)
Tv
Td
Tw
q
q (g/kg)
400
W (mps)
HOLES VISIBLE
THROUGH BOTTOM
OF CLOUD
T.I.
400
—DISTANCE, METERS—

FIG. 8

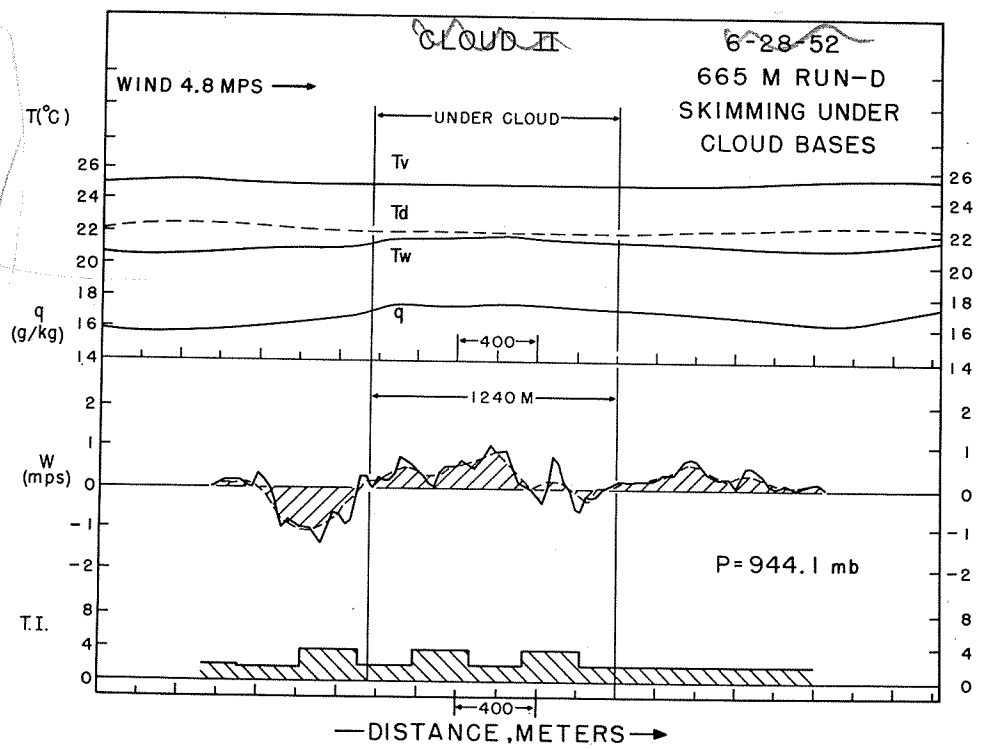
CLOUD II
6-28-52
665 M RUN-D
SKIMMING UNDER
CLOUD BASES
WIND 4.8 MPS
UNDER CLOUD
T(°C)
Tv
Td
Tw
q
q (g/kg)
400
1240 M
W (mps)
P=944.1 mb
T.I.
400
—DISTANCE, METERS—

FIG. 9

TABLE I - ENTRAINMENT

Level m	Pressure mb	$\bar{T}$ draft °C	$\bar{q}$ draft gm/kg	T env. °C	q env. gm/kg	$\frac{\Delta M}{M_o}$	$\frac{1}{M}\frac{dM}{dz} \times 10^5$ cm-1	Increment of liquid water gm/kg	Wind shear mps/km
665	944.1	22.1	17.4	22.2	17.0				
830	926.0	20.5	16.6	20.6	15.8 to 16.0	1.0 to 1.2	6.0 to 7.6	0 to minus trace	3.65
988	909.2	19.5	16.0	20.4	14.0 to 14.8	.23 to .47	1.4 to 3.0	0.1 to trace	-1.90
1108	895.8	18.95	15.5	19.0	13.5 to 14.5	.12 to .23	1.0 to 1.95	~ 0.25	-1.66
1296	876.2	17.9	14.8	17.6	13.7 to 14.2	.33 to .60	1.8 to 3.2	0.50 to 0.40	-6.00
1522	853.5	16.1	13.5	15.8	12.5 to 12.8	1.0 to 1.4	4.4 to 6.1	0.40 to 0.30	-6.00

The range of values in the mixing ratio of the environment, q_{env}, is not due to instrumental uncertainty but to the fact that on one side of the updraft was clear air and on the other side was moister cloudy air. The extreme range was therefore considered. This gives rise to a range in entrainment, as shown. The bars above the draft temperatures, $\overline{T}$ draft, and mixing ratios, $\overline{q}$ draft, signify that means were taken graphically across the horizontal extent of the draft. M stands for mass flux, where $\overline{M}$ is the average value of the flux between the two levels considered. The values of $1/\overline{M}$ dM/dz are quite comparable to those obtained from the work of Stommel (1947; see also Malkus, 1952b). The large values at the lowest and uppermost levels of the cloud will be elucidated in Table III, when dynamic entrainment is compared to gross entrainment.

b. Draft calculation

Table II gives the draft calculation based on equation (7). The virtual temperatures and draft diameters were taken from Figures 4-9. The cross-sectional draft area was obtained by assumption of circular drafts. The $\overline{w}_o$ at 665 m represents the graphically averaged (across the draft diameter) observed draft speed at that level. The values of buoyancy, α, contained in the parentheses are means between each of the two successive levels. The densities, ρ, were calculated from the equation of state and all the remainder of the quaintities except the parcel T_v by successive applications of equation (7). The virtual

TABLE II - DRAFT CALCULATION

Level	Pressure	$\rho \times 10^3$	T_v parcel	$\bar{T}_v$ draft	$\bar{T}_v'$ env.	a	Draft diameter	$\frac{1}{\bar{A}} \frac{dA}{dz} \times 10^4$	$\bar{w}_o$	$a/\bar{w}_o^2 \times 10^4$	Δw	$\bar{w}$
m	mb	gm/cm^3	^oK	^oK	^oK	cm/sec^2	m	cm^{-1}	cm/sec	cm^{-1}	cm/sec	cm/sec
665	944.1	1.104	298.1	298.1	298.1	0	(2 drafts) 820	0	40	2.07	68	
830	926.0	1.088	297.9	296.5	296.3	(.331) .662	(2 drafts) 820		108			108
988	909.2	1.071	297.1	295.8	295.55	(.742) .822	640	-.298	188	.638	80	188
1108	895.8	1.06	296.6	294.8	294.7	(.577) .332	700	.122	192	.162	4	192
1296	876.2	1.04	295.8	293.6	292.6	(1.87) 3.42	800	.142	260	.510	68	260
1522	853.5	1.02	294.9	291.5	290.9	(2.72) 2.02	960	.160		.400	70	330

temperature which would be characteristic of the unmixed parcel, T_v(parcel), was obtained from an adiabatic diagram, using the moist adiabat which intersects the sounding at cloud base.

Table III shows the comparison between the calculated mean draft speed, $\overline{w}$, in Table II and the observed $\overline{w}$, obtained from Figures 4-9 by averaging graphically across the draft diameter at corresponding levels. Other comparisons of interest, such as that between gross and dynamic entrainment, are also shown.

It is important to note the very good agreement between calculated and measured updraft speeds. With the exception of the 1108 m level, the departures between observed and calculated values do not exceed 28 cm/sec, which is within the accuracy of the draft observations. As for the 1108 m level, the columns showing total and dynamic entrainment and mass flux may indicate that the measured draft speed at that level is erroneously low. If the airplane were diving rather than levelled out when the run was begun, or if it departed from constant attitude during the run, such an error could have resulted. By commencing the integration later, rather than at the point on the accelerometer record marked "start", higher draft velocities would have been obtained. This, however, represents a departure from the strictly objective way in which all the remaining data were reduced and therefore seems undesirable, especially since corrections for attitude variations and accurate zeros will be obtained on all future flights.

TABLE III - COMPARISONS

Level m	Calc. $\bar{w}$ cm/sec	Obs. $\bar{w}$ cm/sec	Parcel $\bar{w}$ cm/sec	Mass flux calc. $\bar{w}$ $\times 10^8$ gm/sec	Mass flux obs. $\bar{w}$ $\times 10^8$ gm/sec	Dynamic Entrain. calc. $\bar{w}$ $\times 10^5$ cm^{-1}	Dynamic Entrain. obs. $\bar{w}$ $\times 10^5$ cm^{-1}	Gross Entrainment $\times 10^5$ cm^{-1}	Difference gross minus dyn. $\times 10^5$ calc. $\bar{w}$	Difference gross minus dyn. $\times 10^5$ obs. $\bar{w}$	Shear mps/km
665	(40)	40	(40)		2.34						
830	108	80	1070	6.15	4.56	5.4	3.9	6.0 to 7.6	0.6 to 2.2	2.1 to 3.7	3.65
988	188	200	1147	6.46	6.88	0.3	2.6	1.4 to 3.0	1.3 to 2.7	-1.2 to 0.4	-1.90
1108	192	120	1207	7.82	4.90	1.6	-2.8	1.0 to 1.95	-0.6 to 0.35	3.8 to 4.7	-1.66
1296	260	270	1334	13.60	14.11	2.9	5.1	1.8 to 3.2	-1.1 to 0.3	-3.3 to -1.9	-6.00
1522	330	325	1563	24.36	23.80	2.5	2.3	4.4 to 6.1	1.9 to 3.6	2.1 to 3.8	-6.00

The third column from the left shows the vertical ascent rate of an unmixed parcel rising moist adiabatically from cloud base. Its speed was calculated from equation (6) using a $\overline{w}_o$ of 40 cm/sec at cloud base. At the highest level studied, 1522 m (see Figure 9), the unmixed parcel would have an upward speed of over 15 m/sec, nearly five times the observed and calculated mean draft speeds, which almost exactly coincide. Since the accelerometer records were read at one-half second intervals (~25 m distance intervals), bubbles this size or larger rising nearly unmixed from cloud base are almost surely precluded. (Scorer and Ludlam, 1953). A detailed comparison (see Brewer, 1953) of the water column accelerometer used in this study with a highly sensitive electric accelerometer (response better than 1/60 second) and with a direct study of the gust loads imposed on the aircraft wings demonstrates conclusively that if such fluctuations had existed, they would have been detected by the present method.

It is also interesting to note the consistency between the dynamic entrainment calculated from the relation $M = \rho A w$ and the gross entrainment calculated from psychrograph measurements. The high value of gross entrainment between cloud base and 830 m is seen to be nearly equalled by the influx required to meet continuity. The fact that the mass flux increases by a factor of two or three between 665 m and 830 m indeed supports earlier ideas that trade cumuli get most of their air from within the cloud layer and not from the subcloud layer.

The level at which the gross entrainment greatly exceeds dynamic entrainment is the topmost (1522 m), where the wind shear is very large and the cloud has a pronounced backslant. This implies that the "detrainment" is largest here, or that the air is moving most rapidly through the cloud, as hypothesized previously by Malkus (1952a). The average rate of detrainment, $1/\overline{M}_o \, dM_o/dz$, is 1.3×10^{-5} cm^{-1} (the average of the figures in the second and third columns from the left in Table III). If we find $\overline{M}$, the average mass flux in the cloud from averaging the fourth column from the right, as 10.1×10^8 gm/sec, and take the total height through which the cloud has risen to be 1340 m, the total mass flux detrained turns out to be 1.74 times the average mass flux in the cloud or 17.6×10^8 gm/sec detrained. If it can be thought that the influx occurs largely on the upshear side of the draft, and the efflux on the downshear side, this represents an average rate of flow of air "through" the draft of the order of a meter per second. In other words, the implication is that about 800 sec (or 13 min) would be required for air to travel all the way through the cloud horizontally. If a hypothetical bunch of molecules started on the upshear edge of the draft at its base and rose at the average rate of ascent, this is just the time that they would require to reach the cloud top. Due to the extremely violent mixing within the cloud, it is highly unlikely, however, that such aggregates could retain their identity. This contention is supported by the fact that at the top level, for example, the <u>maximum</u> observed virtual temperature is 292.2 °K, while the virtual

temperature pertinent to an unmixed parcel would be 294.7 °K, an excess of 2.7 °K! Although the assumption of saturation within the clouds might at some levels lead to underestimation of cloud temperatures by one or two tenths of a degree, undetected significant-sized fluctuations of the order of a degree or more can be precluded.

It would further appear from Table III that a vertical component of form drag is probably negligible, since the calculated vertical motions show no tendency systematically to exceed those observed. This is indeed to be expected in the quasi-steady phase of a cumulus cloud's life cycle. It has been pointed out by Schmidt (1947) that form drag in the vertical would be caused by the subtraction of energy from the updraft to establish a counter-current or compensating downdraft. This current, if existant, should be well established by the time the cloud has reached the quasi-steady condition of the present one.

c. Slope calculation

The slope of the draft in the plane of the wind may now be calculated using the method of Malkus (1952b). The results of this calculation are presented in Table IV.

This computation involved obtaining the relative cloud-air horizontal velocity, $u_c - u_E$, at each level. This quantity is positive when the cloud moves downwind faster than the external wind, u_E, and was assumed to be zero at draft base (665 m), implying that the draft had no roots below cloud base. As was demonstrated earlier by Malkus (1952b), $u_c - u_E$ depends critically

TABLE IV - SLOPE CALCULATION

Level m	$\frac{1}{\bar{M}}\frac{dM}{dz} \times 10^5$ cm-1	$u_E - u_{oE}$ cm/sec	$u_c - u_E$ cm/sec	$u_c - u_{oE}$ cm/sec	$\bar{w}$(calc.) cm/sec	Slope = $\frac{\bar{w}(calc.)}{u_c - u_{oE}}$	Slope using mean $\frac{1}{\bar{M}}\frac{dM}{dz}$
665							
	6.0 to 7.6						
830		59.4	-38.2 to -34.2	21.2 to 25.5	108	5.1 to 4.3	4.5
	1.4 to 3.0						
988		30.0	- 4.1 to 2.9	26.0 to 33.0	188	7.2 to 5.7	6.2
	1.0 to 1.95						
1108		10.0	15.3 to 20.4	25.3 to 30.4	192	7.6 to 6.3	6.7
	1.8 to 3.2						
1296		-100.0	106 to 95.5	3.0 to - 7.5	260	86 to -35	∞
	4.4 to 6.1						
1522		-240.0	125 to 97.5	-115 to -142.5	330	- 2.9 to - 2.3	-2.6

on the horizontal resistance forces operating upon the cloud. Table IV is calculated using the assumption that entrainment serves as the only horizontal resistance. The ranges given in cloud-air velocity, $u_c - u_E$, and in departure of cloud (draft) horizontal velocity from the windspeed at cloud base, $u_c - u_{Eo}$, and thus in slope, are due to possible ranges in the proportional rate of entrainment, $1/\overline{M}\ dM/dz$, which has been discussed previously.

Inspection of the column in Table IV marked $u_c - u_E$ shows that the horizontal motion of the draft is downwind slower than the outside air at 830 m, nearly the same as the outside air at 988 m, and faster than the wind at each higher level. The relative cloud-air velocities are fairly large, equalling or exceeding 1 mps at the two upper levels.

The slope calculated in the last right-hand column of Table IV is plotted on the silhouette of the cloud which was given in Figure 3. Figure 10 shows a more detailed consideration of slopes. The two light solid lines to right and left of the heavy curved solid line show the range in slopes indicated in the next-to-last column of Table IV. It was also desired to gauge the effect of additional resistance forces in the horizontal, such as form drag, upon the slope. The dashed lines in Figure 10 show the slope the draft would exhibit at each level if an additional resistance were operative, equivalent to a proportional entrainment rate of 2×10^{-5} cm^{-1} (see Malkus, 1952b, equation (13) and discussion; also section 2b) in addition to the maximum

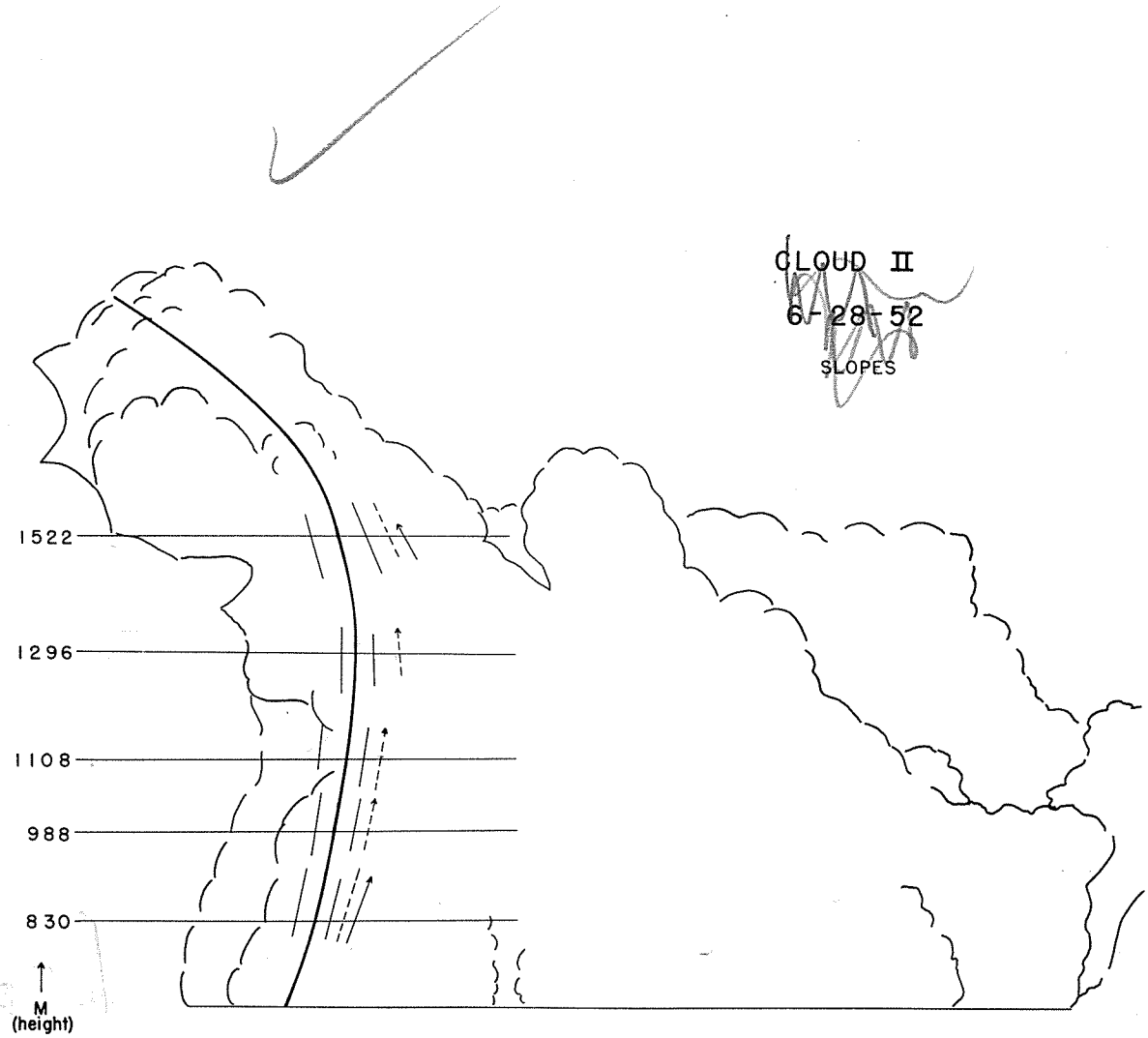

FIG. 10

entrainment rate of Table IV. The arrows at the extreme right in Figure 10 show the slope at each level that would obtain if the resistance represented by the mean entrainment were doubled, thus allowing for a form drag resistance force equal to that provided by entrainment. Although at 830 and 1522 m, the cloud does not slant as much as the arrows, a slope drawn through the dashed lines clearly is not precluded. Thus a horizontal form drag coefficient of 2×10^{-5} cm^{-1} or somewhat larger may have been operative. Since the cloud slant is only slightly altered by rather large changes in horizontal resistance, it probably will not be possible to pin down the resistance any more accurately than this by the slope method.

d. Correlations

Finally, some correlations are of interest. In Figures 4-9, values of "turbulence index", or the relative development of small-scale turbulence, were plotted. This index was obtained by planimetering the envelope of the water column accelerometer over distance intervals of about 240 m. To test the often-used assumption that high roughness or turbulence index is associated with active updrafts, the correlation was made between the average draft over each 240 m interval and the corresponding turbulence index. This was done for each run shown in Figures 4-9. Where the sign of the drafts was considered, downdrafts being called negative, the correlation for Cloud II and its environment came out +0.49. When only the magnitudes of the drafts were considered, the

correlation was +0.71.

It has, in contrast, been contended that the roughness in cumulus clouds should be more associated with horizontal shear in vertical drafts, rather than simply with the drafts themselves. Consequently a correlation was taken between the turbulence index and the average horizontal shear in the drafts for the corresponding interval. This correlation proved to be +0.82. For the same distance intervals, a third correlation was made between average draft magnitude and the average magnitude of their horizontal shear. This correlation came out +0.73. Seventy-two pairs of numbers were used in obtaining each of these correlations. Concerning the significance of the resulting coefficients it may be shown (see Fisher, 1941) that seventy-two pairs of random numbers would have to be correlated 100 times before a correlation as high as +0.30 would arise by pure chance. The difference between correlation coefficients of +0.71, +0.82, and +0.73 cannot, however, be regarded as significant. Therefore, it may be inferred that a good rule of thumb to locate cloud-scale drafts is the development of roughness in and around clouds, though this method does not appear to select updrafts per se.

Concerning the cause of cumulus roughness, only a clue is provided. In view of the high correlation between drafts, regardless of sign, and draft shear and to the relatively poorer correlation between updrafts and roughness, evidence is provided in favor of the contention that the turbulence is caused mechanically by shear rather than by the release of latent heat or by

some other process directly associated with ascent. Further information on this topic is provided in the discussion of Cloud I to follow.

V CLOUD I - JUNE 28, 1952

This cloud, photographed in the plane of the wind, is shown in Figure 11. It is the largest member of a cluster of clouds. The airplane was able to complete seven traverses through the cloud in twenty minutes, at the end of which its appearance had changed relatively little. A summary of the draft structure within this cloud is shown in Figure 12, with the exception of the run made at 1450 m, which was not flown quite along the same course. It was possible to construct only the upper part of the cloud silhouette (containing the topmost two runs) from the photograph; the rest of the cloud has been put together using the slope which was later calculated from the data. The individual runs, from top to bottom, are shown in Figures 13-19.

It is interesting to note that the drafts in this cloud also appear to break up into separate "cells" as the 830 m level is reached. It was at this level that the observer began to record vertical holes in the cloud, which permitted the sea surface to be seen clearly although the airplane was still surrounded horizontally by cloud matter. This cloud was clearly in a later stage of its life cycle than Cloud II, exhibiting only downdrafts on the uppermost run and a very strong downdraft, of nearly 4 mps, on the next-to-uppermost run at 1554 m. It therefore seemed very

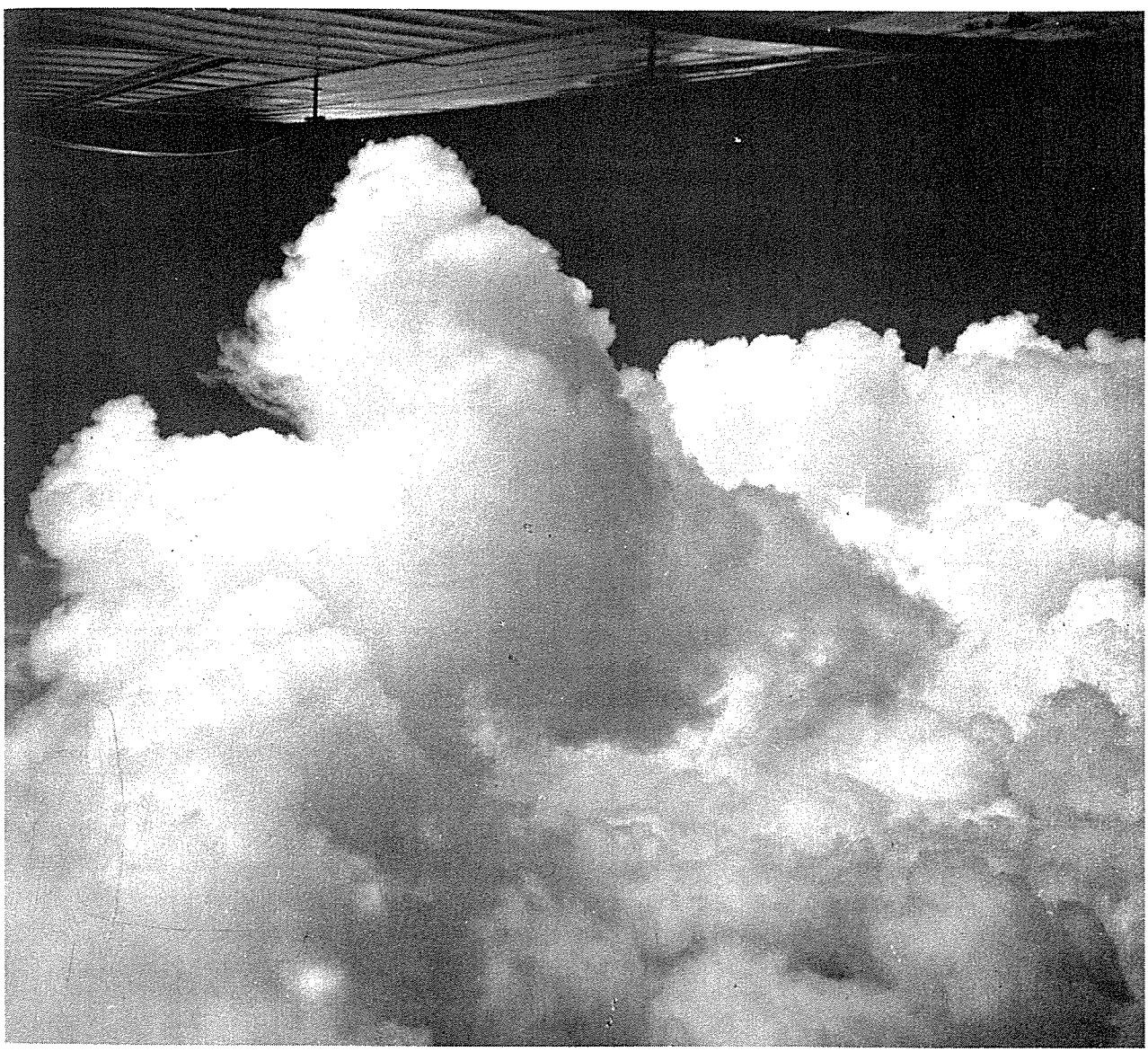

FIG. 11

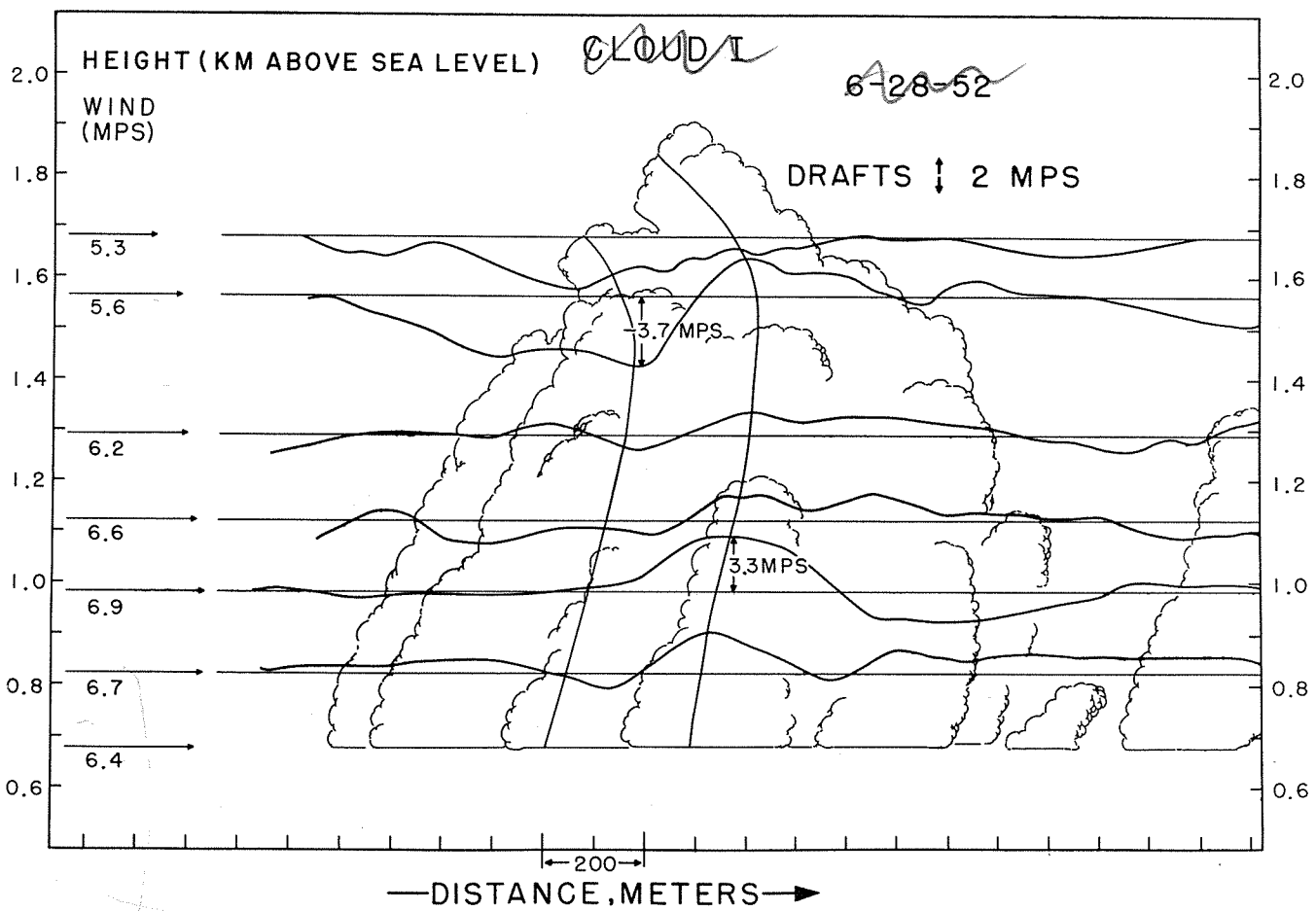
HEIGHT (KM ABOVE SEA LEVEL)
CLOUD I
6-28-52
WIND
(MPS)
DRAFTS ↕ 2 MPS
2.0
1.8
1.6
1.4
1.2
1.0
0.8
0.6
5.3
5.6
6.2
6.6
6.9
6.7
6.4
3.7 MPS
3.3MPS
200
DISTANCE, METERS

Fig. 13

FIG. 12

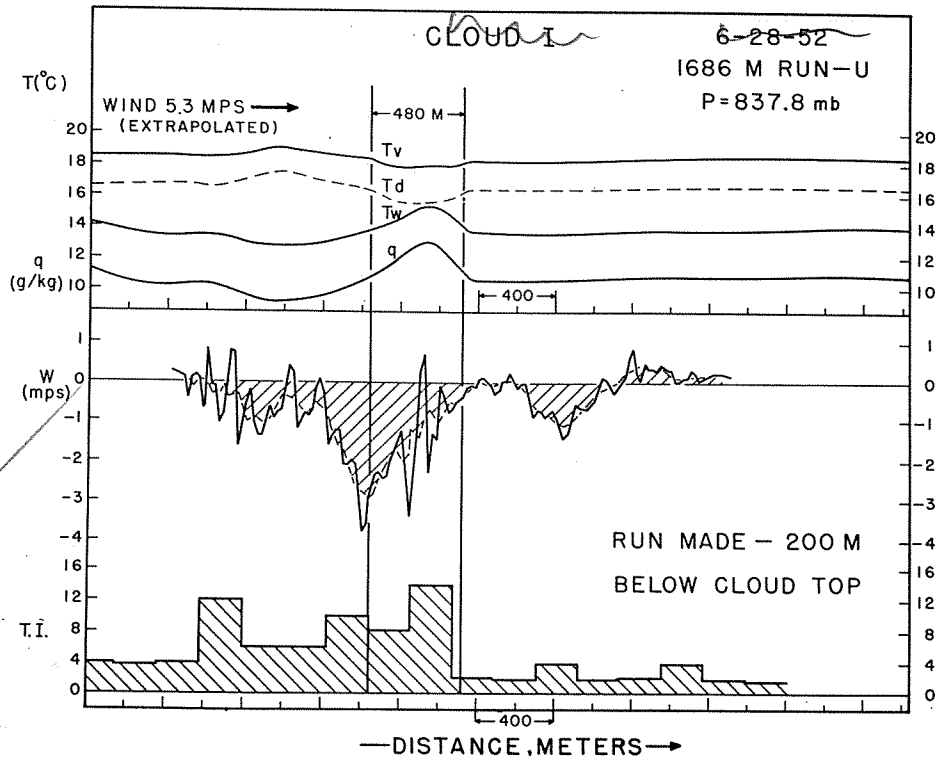

14

FIG. 13

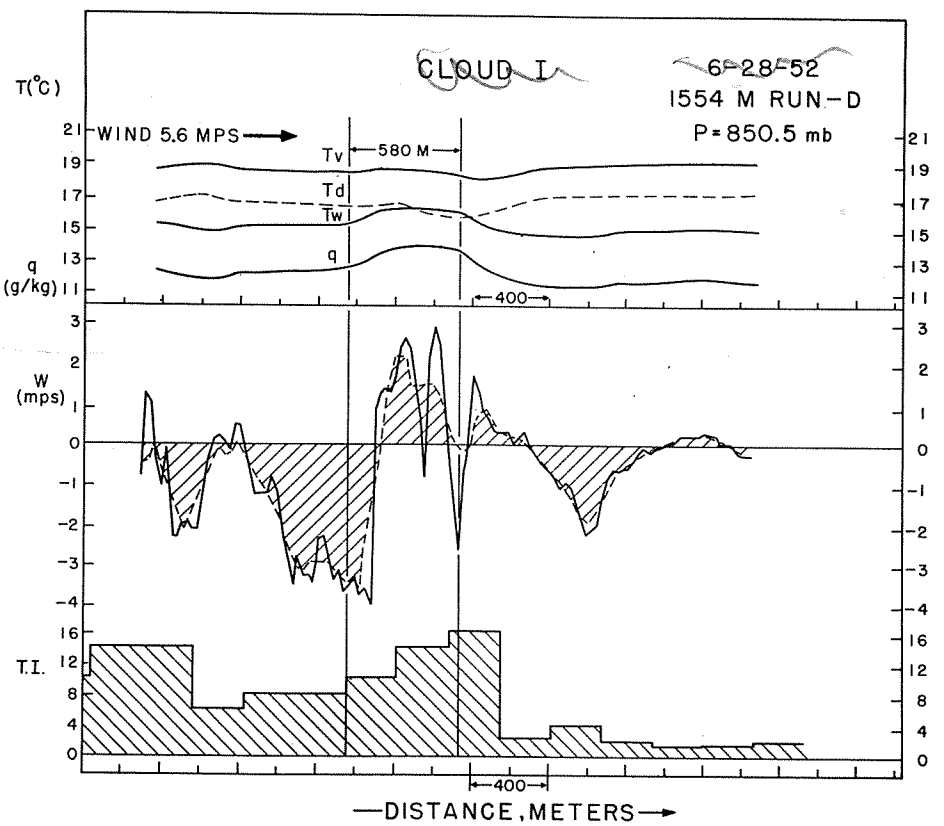

15

FIG. 14

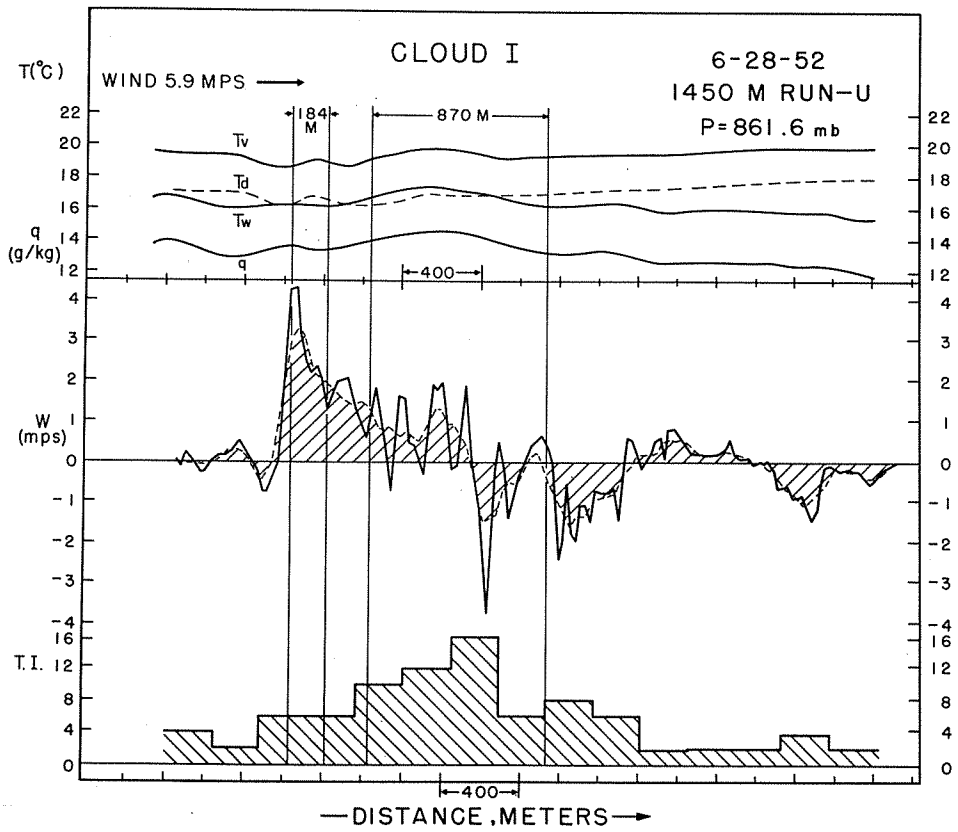
CLOUD I
6-28-52
1450 M RUN-U
P=861.6 mb
WIND 5.9 MPS
T(°C)
184 M
870 M
Tv
Td
Tw
q
q (g/kg)
400
W (mps)
T.I.
400
—DISTANCE, METERS—

FIG. 15

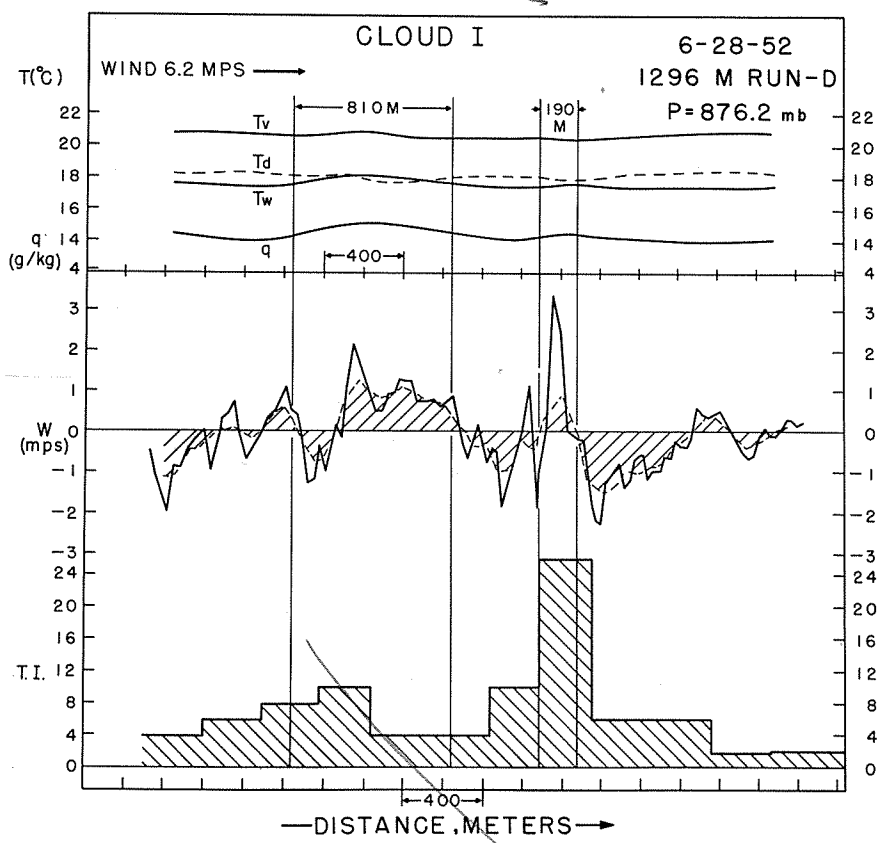
CLOUD I
6-28-52
1296 M RUN-D
P=876.2 mb
WIND 6.2 MPS
T(°C)
810 M
190 M
Tv
Td
Tw
q
q (g/kg)
400
W (mps)
T.I.
400
—DISTANCE, METERS—

FIG. 16

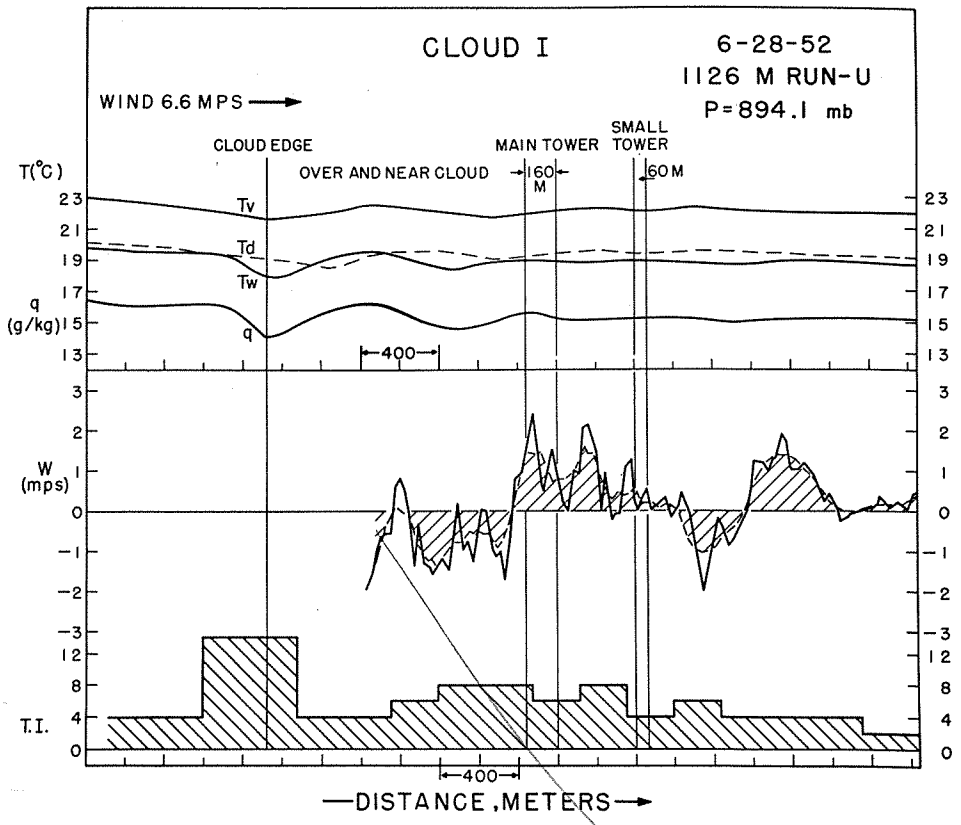
CLOUD I
6-28-52
1126 M RUN-U
P=894.1 mb
WIND 6.6 MPS
CLOUD EDGE
OVER AND NEAR CLOUD
MAIN TOWER
160 M
SMALL TOWER
60 M
T(°C)
Tv
Td
Tw
q
(g/kg)
400
W
(mps)
T.I.
DISTANCE, METERS

FIG. 17

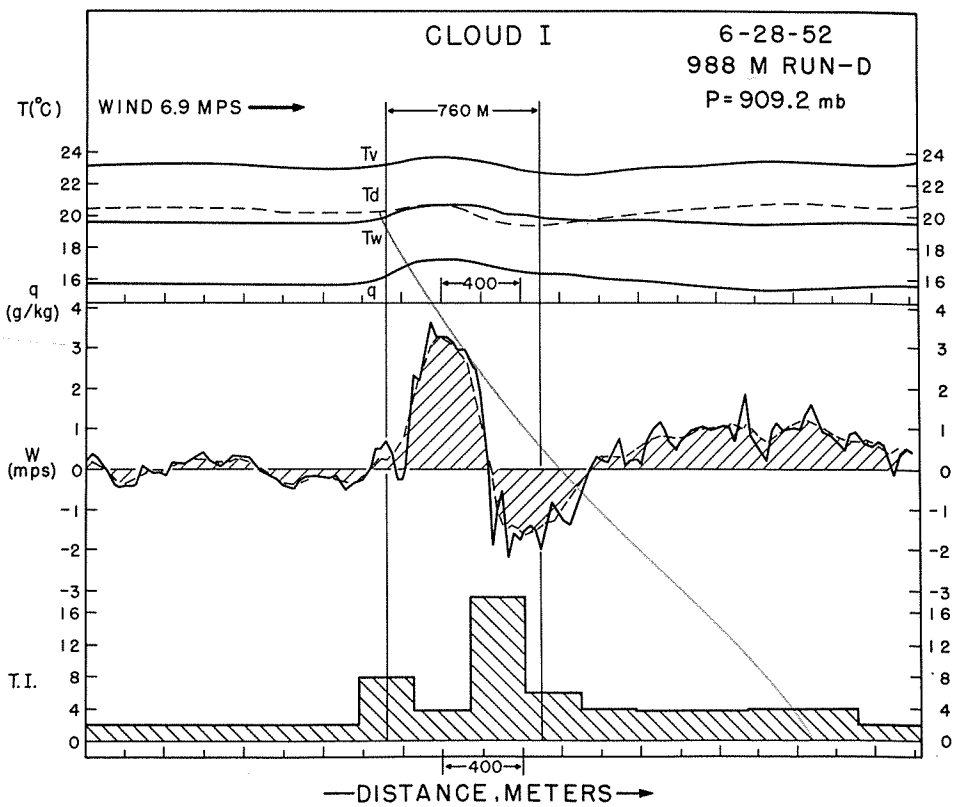
CLOUD I
6-28-52
988 M RUN-D
P=909.2 mb
T(°C)
WIND 6.9 MPS
760 M
Tv
Td
Tw
q
(g/kg)
400
W
(mps)
T.I.
DISTANCE, METERS

FIG. 18

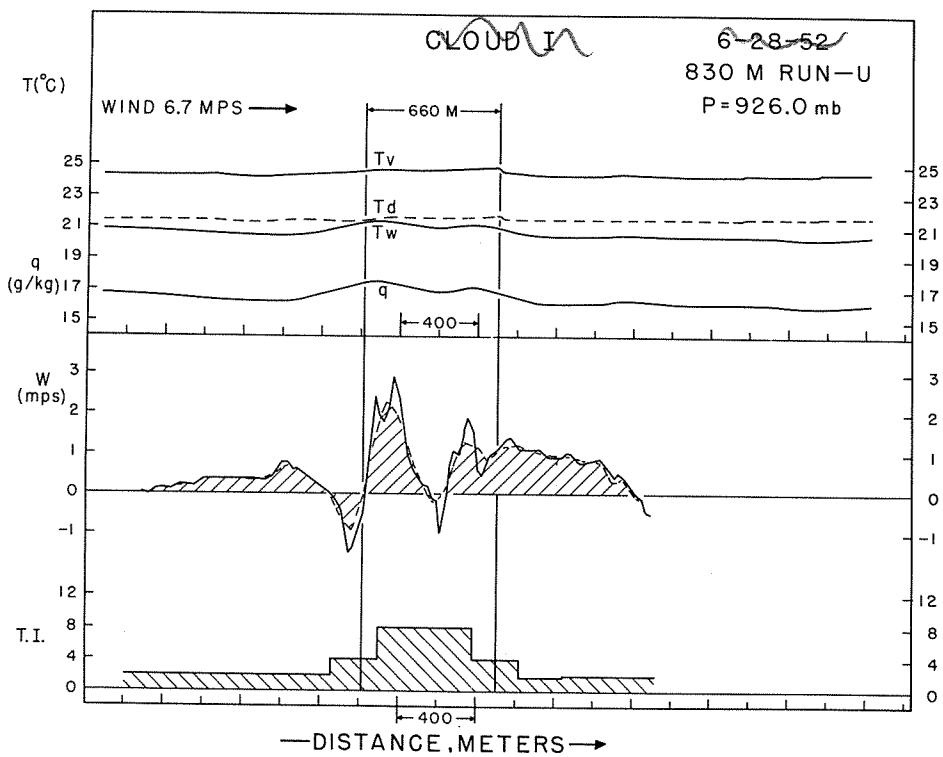
CLOUD I
6-28-52
830 M RUN—U
P=926.0 mb
T(°C)
WIND 6.7 MPS
660 M
Tv
Td
Tw
q
(g/kg)
q
400
W
(mps)
T.I.
400
—DISTANCE, METERS—

Fig. 16

FIG. 19

doubtful at first whether calculations based on the steady-state cloud model would have any meaning in this case. When, however, they were made separately for updraft and for downdraft, it was found that the computed quantities were very consistent and agreed rather well with observed values, although with not such good agreement as was found in the case of Cloud II.

a. Entrainment calculation

The method of calculating entrainment evolved by Stommel (1947) was modified readily to apply to downdrafts and evaporation of liquid water. The downdraft extended from the topmost run at 1686 m perhaps down to 1296 m where it is barely perceptible on Figure 16. In calculating the entrainment from one level to the next lower one, the problem arose that the environment of the downdraft differed radically from relatively dry, clear air on the upwind side to very moist, cloudy updraft air on the downwind side. Various proportions of these two environments were considered to have mixed with the draft and the results are presented in Table V.

The fourth column from the right shows the proportional rate of entrainment between the two levels when the downdraft is entraining entirely updraft (cloudy) air and is not mixing with the clear air at all. The next column to the right shows the proportional rate of entrainment when the draft is entraining equal amounts of air from the clear and from the updraft. The next-to-last right-hand column shows the entrainment rate when

TABLE V - ENTRAINMENT IN THE DOWNDRAFT

Level	$\bar{T}$ downdraft	$\bar{q}$ downdraft	$\bar{T}$ clear	$\bar{q}$ clear	$\bar{T}$ updraft	$\bar{q}$ updraft	$\frac{1}{\bar{M}}\frac{dM}{dz} \times 10^5$ (updraft)	$\frac{1}{\bar{M}}\frac{dM}{dz} \times 10^5$ (mixture)	$\frac{1}{\bar{M}}\frac{dM}{dz} \times 10^5$ (clear)	Evap. Δ
m	°C	gm/kg	°C	gm/kg	°C	°C	cm-1	cm-1	cm-1	gm/kg
1686	16.15	11.5	16.5	10.6	15.8	12.0				
							2	4.4	Impossible	0.3
1554	16.4	12.3	16.8	12.0	16.5	13.6				
							22.2	$\rightarrow \infty$	Impossible	0.2
1296	18.1	14.6	18.2	14.2	18.2	15.0				

all clear air is being entrained. It is immediately evident that the downdraft cannot be mixing solely with clear air, as the calculation shows no possible admixture between clear air and air initially in the draft which can give rise to the observed temperatures and moistures found within the draft at the next lower level. It has been hypothesized by Malkus (1949; 1952a) that air should be moving through the draft in the direction pointed by the shear vector (in this case upwind) and thus that the downdraft should consist primarily of air which was previously in the updraft. The plausibility of this contention is not undermined by the results shown in Table V. It appears from the very large computed value of $1/\overline{M}\ dM/dz$ between the 1554 m level and 1296 m, that at 1296 m the downdraft had either nearly lost its identity or had not yet penetrated.

The last column on the right in Table V gives the quantity of liquid water, in gm/kg, which must have been evaporated from the cloudy downdraft air between successive levels. This varied only negligibly with varying proportions entrained from clear and cloudy air.

The entrainment calculation for the updraft is given in Table VI. The very high calculated proportional rate of entrainment between 988 m and 1126 m is probably due to the fact that on the latter traverse the airplane did not penetrate the center of the cloud (from observer's notebook). The point on the temperature-mixing ratio graph (see Stommel, 1947) for 1126 m was not on a smooth curve including the other updraft points and lay considerably

TABLE VI - ENTRAINMENT CALCULATION FOR THE UPDRAFT

Level m	Pressure mb	$\bar{T}$ updraft °C	$\bar{q}$ updraft gm/kg	$\bar{T}$ env. °C	$\bar{q}$ env. gm/kg	$\Delta M/M_o$	$\frac{1}{\bar{M}} \frac{dM_i}{dz} \times 10^5$ cm-1	Increment of liquid water gm/kg	External shear mps/km
830	926.0	21.55	17.25	21.5	16.1 to 16.8				
988	909.2	20.55	16.8	20.2	16.0 to 16.5	.29 to .78	1.8 to 4.9	0.2	2.3
						1.69 to 5.0	12 to 36 (2 to 4)	0.1 (0.2)	-2.2
1126	894.1	19.25	15.4	19.25	14.6 to 15.1				
1296	876.2	18.0	14.95	18.2	14.0 to 14.2	.37 to .44	2.2 to 2.6	0.2	-2.2
1450	861.6	17.2	14.4	17.1	13.2 to 14.0	.24 to .41	1.5 to 2.7	0.35	-2.2
1554	850.5	16.3	13.7	16.5	12.0 to 12.4	.36 to .47	3.6 to 4.5	0.30	-2.4
1686	837.8	15.8	12.0	16.4	10.6	1.18	9.0	0.15	-2.4*

* extrapolated above 1600 m

nearer the outside air curve. If the corresponding point on the smooth curve for the updraft was taken as giving better values for the T and q of the draft at 1126 m, the entrainment rate becomes that indicated in the parentheses; namely, 2 - 4×10^{-5} cm^{-1}, which is in good agreement with the other calculated values in the column. At the topmost level of cloud penetration, 1686 m, the updraft had dwindled to zero and hence there was little or no ascending mass flux through that level. This fact is reflected in the very high calculated entrainment rate, showing that a high proportion of environment air had mixed with the draft, the identity of which was rapidly becoming lost.

b. Draft calculation

Table VII gives the draft calculation for the downdraft, based on equation (7). It is seen that the observed virtual temperatures and draft diameters give rise to a downward acceleration of the downdraft between 1686 m and 1554 m which is well within observational error. It is also seen that the entrainment required to fulfill continuity, 1.28×10^{-5} cm^{-1}, is in good consistency with the results of Table V which gave a corresponding gross entrainment between 2 and 4.4×10^{-5} cm^{-1}. The draft calculation for the updraft also gives fairly satisfactory results, as shown in Table VIII.

The run at 1126 m has been omitted from the preceding calculation, due to the fact that the cloud center was not penetrated, as well as the 1450 m run, which was made on a different

TABLE VII - DRAFT CALCULATION FOR THE DOWNDRAFT

Level m	$\bar{T}_v$ draft ^oK	$\bar{T}_v'$ env. ^oK	$\rho \times 10^3$ gm/cm^3	α	Draft diameter m	$\frac{1}{\bar{A}}\frac{dA}{dz} \times 10^4$ cm^{-1}	$\bar{w}_o$ cm/sec	Δw cm/sec	$\bar{w}_{calc.}$ cm/sec	$\bar{w}_{obs.}$ cm/sec	M(obs) x 10^{-8} gm/sec	Dynamic entrainment (obs. M) x10^5 cm^{-1}
1686	291.1	291.5	1.0	-1.37 (-1.02)	800		-160			-160	8.05	
						-.169		-60				1.28
1554	291.5	291.7	1.02	-.675	720				-220	-230	9.54	
1296					200(?)	Draft essentially disappeared						

2 - 30
2 - 4.4

TABLE VIII - DRAFT CALCULATION FOR THE UPDRAFT

Level m	$\bar{T}_v$ draft °K	$\bar{T}_v'$ env. °K	$\rho \times 10^3$ gm/cm^3	α	Draft diameter m	$\frac{1}{\bar{A}} \frac{dA}{dz} \times 10^4$ cm^{-1}	$\bar{w}_o$ cm/sec	Δw cm/sec	$\bar{w}_{calc.}$ cm/sec	$\bar{w}_{obs.}$ cm/sec	M(obs) x 10^{-8} gm/sec	Dynamic entrainment x 10^5 cm^{-1}
830	297.6	297.3	1.085	.99 (1.46)	340		140			140	1.4	
						.262		53				5.1
988	296.6	296.0	1.07	1.94 (0.72)	420		193		193	220	3.25	
						.347		-69				0.85
1296	293.6	293.75	1.04	-0.50 (-.08)	760		124		124	90	4.2	
						-.384		51				-1.74
1554	291.55	291.45	1.02	0.34 (-.52)	440		175		175	170	2.64	
						.835		-118				
1686	291.5	291.7	1.00	-1.37	800				57	-160		

gross

31

1.8 - 4.9

2 - 3

2.5 - 3.5

9.0

heading of the airplane. It is surprising how satisfactorily the steady-state model worked out, even for this cloud. Its deficiency is striking only at the 1686 m level where the departure from a steady-state was most obvious, since the observer noted that the cloud tower was actually descending from one run to the next. The fact that in the lower levels the model appears to be slightly less satisfactory than in the case of Cloud II may well have been due to the fact that Cloud I was a far more difficult cloud to contend with from the airplane pilot's point of view, since it was one of a cluster of several clouds close together.

c. Slope calculation

The slope calculation for Cloud I is shown in Table IX. The slant at 1126 m is probably too great, since the observed $\overline{w}$ of 120 cm/sec was used, which is probably too small since the center of the draft was not penetrated. It was not possible to calculate a slope at 1686 m since no updraft was observed at that level, probably due to the time elapsed (about 3-5 minutes) between the photograph and the 1686 m run. If an average updraft of 50 cm/sec is assumed to have prevailed, the slope comes out about -1.2, in good agreement with the photograph. There is no way of testing the validity of the slope calculation; it was merely used to reconstruct the cloud profile (Figure 12) in those levels not covered by the photograph.

TABLE IX - SLOPE CALCULATION

Level m	$\frac{1}{\bar{M}}\frac{dM}{dz} \times 10^5$ (ave) cm^{-1}	$u_E - u_{oE}$ cm/sec	$u_c - u_E$ cm/sec	$u_c - u_{oE}$ cm/sec	$\bar{w}$(calc) cm/sec	Slope = $\frac{w_{calc}}{u_c - u_{oE}}$
665					0 (assumed)	
	6.7 (from cld II)					
830		37.2	-18.1	19.1	140	7.3
	3.3					
988		60	-28.0	32.0	193	6.0
	3.0					
1126		30	6.4	36.0	120 (obs)	3.3
	2.4					
1296		-10	35	25	124	5.0
	2.8					
1554		-70	61	- 9	175	-19.5
	9.0					
1686		-100	37.2	-62.8	Negative	?

d. Correlations

Finally, the same correlations were calculated for this cloud as for Cloud II, with fairly similar results. The greatest difference arose in the correlation between turbulence index and updrafts, which was only +0.06, in contrast to +0.49 for Cloud II. On the other hand, the correlation between drafts, regardless of sign, and turbulence index, was +0.71, identical with that for Cloud II. The reason for the far lower correlation when signs were considered is that in the two upper levels where downdrafts predominated, the correlation came out -0.65 and -0.11, respectively. This reinforces the conclusion drawn earlier that small-scale roughness (in at least these particular cumuli) is associated mechanically with cloud-scale drafts rather than being related to the condensation process, liquid water, or some parameter peculiar to ascending motion.

Also, similarly to Cloud II, the correlation between turbulence index and horizontal shear in drafts came out +0.76 and the correlation between average draft magnitudes in distance intervals of 240 m and the average draft shear in these intervals came out +0.63, again supporting the remarks made in connection with Cloud II.

VI COMPARISON OF THE TWO CLOUDS AND THEIR ENVIRONMENTS

Cloud I was studied at 1500 Local Standard Time and was located about 10 miles Southwest of St. Croix, V. I. Cloud II was studied at 1630 Local Standard Time and was located about 30

miles Southwest of St. Croix. About halfway between the two cloud investigations in both time and space, a clear air spiral sounding was made, at 1535 L.S.T. and 20 miles Southwest of St. Croix. The wind directions between one and five thousand feet ranged between 140° and 110° on this particular afternoon, hence the air in the area studied cannot have been affected by flow over the island.

The clear air sounding is reproduced in Figure 12, and is quite typical of the area for June. The termination of the smaller clouds at about 1100 m and the relative weakness at that level of the two clouds described here becomes understandable in terms of the rather stable, dry air layer occurring at that height.

It was desired to test how nearly the clear air immediately adjacent to Cloud I and Cloud II resembled the clear air sounding in temperature and moisture content. For that reason the environment temperatures and moistures of Cloud I are plotted as dark triangles on Figure 20, while the values immediately adjacent to Cloud II are indicated by crosses at the appropriate levels. The environment of Cloud II, it will be noted, differs imperceptibly from the clear air sounding, except for the reduction of the extremely dry wafer at 1100 m. This appears to indicate that Cloud II is the first tall cloud to grow in its locality, a supposition which is supported by its isolation. The environment of Cloud I, on the other hand, is both warmer and wetter than the air penetrated by the sounding, and the excessive moisture up to 1450 m is its striking feature. This might indicate that predecessors of Cloud I had wetted the air in that locality, thus

must change legend

CLEAR AIR SOUNDING

6-28-52

(3:35 PM – 20 MI. S.W. OF ST CROIX)

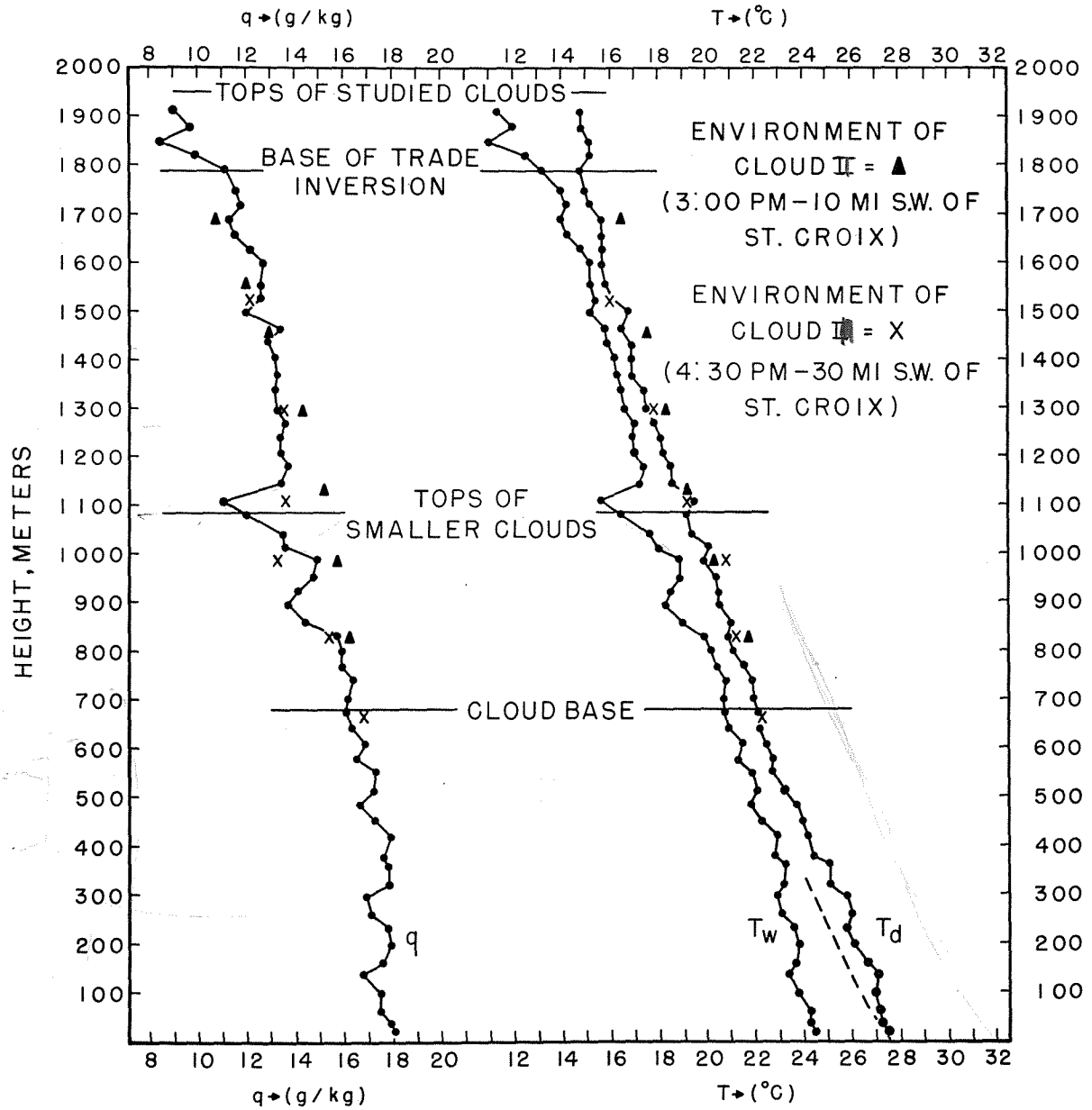

17

FIG. 20

cloud draft structure by means of a slow-flying aircraft can, after considerable pains, be made to work. Furthermore, the adequacy of the several instrumental procedures is indicated by the very consistent picture produced by the meshing of several completely independent measurements. It can be demonstrated that if any of the measurements had been seriously in error, no such coherent structure for these two clouds could have appeared.

The second conclusion concerns confirmation of preceding theories involving cumulus clouds. It appears that the Stommel-Malkus steady-state model is applicable at least to some clouds, and has led to self-consistent, realistic results. The predictions pertaining to entrainment, cloud slopes, lack of trade cumulus "roots", and asymmetries in updraft structure related to wind shear appear to verify, although more observational evidence is still desirable.

Finally, certain suggestions are provided by the data which may contribute eventually to the evolution of a time-dependent cumulus cloud model. The most striking of these appears to be the interaction of cumuli, both in space and in time. In other words, the formation of a very large cloud seems to imply the aggregation of several small neighboring clouds and also the precedence in time of earlier cloud towers in the same locality.

ACKNOWLEDGEMENTS

The writer desires to emphasize the degree to which the present study is the result of a cooperative venture between many persons. Vitally important were the studies of the flight characteristics of the airplane by Given A. Brewer; the instrumentation, largely developed and executed by Kenneth McCasland; the maintenance and skillful flying of the aircraft under Chief Pilot Norman Gingrass; and the photography carried out by Claude Ronne.

In the reduction and analysis phase, valuable computational work was done by Miss Martha A. Walsh and Mrs. Mary C. Thayer; the diagrams represent the drafting skill of Frank Bailey; and the manuscript was prepared by Mrs. Phyllis Casiles.

Last but not least, the writer gratefully acknowledges the contribution made at all stages of the effort by her colleague, Andrew Bunker, without whose participation the work could not have been accomplished.

REFERENCES

Braham, R. R., 1952: The water and energy budgets of the thunderstorm and their relation to thunderstorm development. J. Meteor., 9 (4): 227-242

Brewer, G. A., 1953: Predicting wing lift loads PBY-6A from accelerometer measurements. Ref. No. 53-1, WHOI Tech. Rep. No. 21, Submitted to Office of Naval Research under Contract N6onr-27702 (NR-082-021). 15 pp.

Bunker, A. F., 1953: Investigations into a method of shearing stress determinations from an airplane in flight. Manuscript to appear as a WHOI Technical Report of this project.

Fisher, R. A., 1941: Statistical methods for Research Workers. Oliver and Boyd, Edinburgh, Eighth Edition: 344 pp.

Houghton, H. G. and H. E. Cramer, 1951: A theory of entrainment in convective currents. J. Meteor., 8 (2): 95-102

Malkus, J. S., 1949: Effects of wind shear on some aspects of convection. Trans. Amer. Geophys. Un., 30 (1): 19-25

Malkus, J. S., 1952a: Recent Advances in the study of convective clouds and their interaction with the environment. Tellus, 4 (2): 71-87.

Malkus, J. S., 1952b: The slopes of cumulus clouds in relation to external wind shear. Quart. J. R. Met. Soc., 78 (338): 530-542

Malkus, J. S. and A. F. Bunker, 1952: Observational studies of the air flow over Nantucket Island during the summer of 1950. Pap. Phys. Ocean. and Meteor., Mass. Inst. of Tech. and Woods Hole Ocean. Inst., 12 (2): 50 pp.

McCasland, K., 1951: Modifications of the airplane psychrograph and adaptation of the humidity strip to airplane soundings. Ref. No. 51-59, WHOI Tech. Rep. No. 12, Submitted to Office of Naval Research under Contract N6onr-27702 (NR-082-021). 10 pp.

Schmidt, F. H., 1947: Some speculations on the resistance to the motion of cumuliform clouds. Med. en Verh. B, The Hague, No. 1. 54 pp.

Stommel, H., 1947: Entrainment of air into a cumulus cloud. J. Meteor., 4 (3): 91-94

Stommel, H., 1951: Entrainment of air into a cumulus cloud II. J. Meteor., 8 (2): 127-129

TITLES FOR ILLUSTRATIONS

Fig. 1. Schematic diagram illustrating the manner in which the cumulus clouds were traversed by the PBY. One earlier run was made (usually flying downwind) past the cloud at a distance from it of 4-5 miles so that the cloud could be photographed in the plane of the wind. The topmost run was made at the same level at which the photograph was taken.

Fig. 2. Photograph, in the plane of the wind, of Cloud I. The wind blows from left (East Southeast) to right across the picture.

Fig. 3. Summary of the data taken for Cloud I, put together with the aid of Fig. 2. The solid curves are vertical draft velocities (running mean values over 150 m distance), with the origin being the thin horizontal line at each level. The dashed lines are temperatures, assuming saturation within the cloud boundaries, so that inside the cloud the wet-bulb temperatures are used; dry-bulb temperatures being represented outside. The x-ed lines are mixing ratios. The figures to the far right are the environment wet-bulb temperature, mixing ratio, and dry-bulb temperature, respectively. The latter two are taken as the values of the origins of the x-ed and dashed curves. The calculated (see Table IV) slope of the cloud is given by the heavy curved line. The winds obtained by double

drift of the aircraft are shown by the arrows at the extreme left. Note the separation of the drafts into "cells" at the 830 m level, where one of the large vertical holes in the cloud is indicated.

Fig. 4. The 1522 m run through Cloud II. U designates the fact that it was flown in the upwind direction (from right to left). The solid vertical lines 1540 m apart designate that part of the record actually within the liquid cloud. T_v stands for virtual temperature; T_w for wet-bulb temperature; T for dry-bulb temperature; q for mixing ratio. The curves marked w are vertical velocities, the solid curve being composed of values found from integrating accelerations read off every 25 m; the dashed (shaded) curve being running averages of six of these values, or 150 m averages. The bottom curve, T.I., is turbulence index and the numerical values are of significance only relative to each other. Note that shortly after entry into the cloud the dry-bulb temperature becomes lower than that of the wet-bulb. This results from a wetted dry-bulb upon the readings of which the dry dynamic correction is still applied. Within the cloud, the dry- and wet-bulb temperatures were assumed equal and the wet-bulb curve was used to obtain mixing ratio and virtual temperature. Also note the single smooth peak of the temperature and mixing ratio within the cloud and the flatness of these curves outside the cloud boundaries.

Fig. 5. The 1296 m run through Cloud II. Notation same as Fig. 4, except that D stands for the fact that the run was flown in the downwind direction (from left to right). Note that another smaller cloud tower was passed over, indicated by the shorter pair of vertical lines.

Fig. 6. The 1108 m run through Cloud II. Notation same as Fig. 4.

Fig. 7. The 988 m run through Cloud II. Notation same as Fig. 4.

Fig. 8. The 830 m run through Cloud II. Notation same as Fig. 4. Note that the updrafts are separated into separate "cells" at this level and so are the peaks in the temperature and moisture records. Note also the greater "waviness" of the latter records outside of the cloud boundaries. The value 24 of turbulence index associated with the left-hand cloud draft is one of the highest values observed during the 1952 trip.

Fig. 9. The 665 m run just under the base of Cloud II (in clear air skimming cloud bottom). Notation same as Fig. 4, except that the vertical lines define that part of the record made directly under, rather than within, the cloud. Note the extreme flatness of the T_v curve, showing no buoyancy whatsoever beneath the cloud. There is also no excess turbulence beneath the cloud and no "roots" of any kind are detectable.

According to Bunker[2] vertical drafts of 40-60 cm/sec are the rule not the exception in the clear air away from clouds at this level.

Fig. 10. Schematic diagram of varying slopes for Cloud II. The heavy solid curve is the slope given by the last column on the right in Table IV. The light solid lines on either side of this curve are the slopes shown in the next-to-last right-hand column of Table IV; that is to say, the possible range due to the possible range in entrainment rates (depending on the relative entrainment from the two sides of the draft). The dashed line is the slope which would obtain at each level if an additional resistance equivalent to a proportional entrainment rate of 2×10^{-5} cm^{-1} were added to the maximum entrainment rate shown in the next-to-last column of Table IV. In other words, the dashed lines represent the slope the draft would have if, in addition to the maximum amount of mixing, a form drag force of a sizeable amount were added. The arrows show the slope which would obtain if the mean entrainment rate were doubled, or if a form drag force were added which was just as great as the resistance due to the mean value of the entrainment. Where the dashed lines and the arrows would very nearly coincide they are indicated by a single dashed arrow. The cloud silhouette in the background is drawn to scale from the photograph.

---

[2] Conversation with the author.

Fig. 11. Photograph in the plane of the wind of the upper portions of Cloud I. The wind blows from left (East Southeast) to right across the picture.

Fig. 12. Summary of the draft structure for Cloud I, put together at upper levels with the aid of the photograph (Fig. 11) and at lower levels by using the computed slope. The solid curves are the drafts when a running average over 150 m distances are taken. The origin is the thin horizontal line at each level. Note the predominance of downdrafts in the upper levels.

Fig. 13. The 1686 m run through Cloud I. Notation the same as Figs. 4-9. Note the lower virtual temperature (negative buoyancy) within the cloud.

Fig. 14. The 1554 m run through Cloud I. Notation the same as Figs. 4-9. This downdraft (nearly 4 mps) was the strongest observed on the 1952 trip.

Fig. 15. The 1450 m run through Cloud I. Notation the same as Figs. 4-9. This run was omitted from Fig. 11 and from the draft calculations since it was flown along a slightly different course from the rest.

Fig. 16. The 1296 m run through Cloud I. Notation the same as Figs. 4-9. Note the strong draft and turbulence in the

smaller cloud to the right (downwind) of the main cloud.

Fig. 17. The 1126 m run through Cloud I. Notation the same as Figs. 4-9. It is readily seen that the cloud and draft center were not penetrated by this run. After flying through a small tower (60 m diameter) the pilot entered the main tower, flying upwind, but emerged after only 160 m. From there to the line marked "cloud edge" the plane was flying beside the main cloud and above lower "outrigger clouds".

Fig. 18. The 988 m run through Cloud I. Notation the same as Figs. 4-9.

Fig. 19. The 830 m run through Cloud I. Notation the same as Figs. 4-9. This was the lowest run made through Cloud I. Note that the draft, moisture, and temperature curves are also starting to separate into "cells" at this level. Holes were seen from here down to the sea surface.

Fig. 20. Clear air sounding made using psychrograph in spiral descent about 2 miles in diameter. T_d denotes the dry-bulb curve; T_w denotes the wet-bulb curve; and the mixing ratio curve is indicated by q. The ordinate gives the height in meters, and the dashed line next to the T_d curve is a dry adiabat.

Technical Report Distribution List
ONR Project NR-082-021

20 March 1953

Address	Copies
Chief of Naval Research, Navy Department, Washington 25, D. C. Attention: Code 416	3
Director, Naval Research Laboratory, Washington 25, D. C. Attention: Technical Information Officer, Code 2000	9
Director, Office of Naval Research Branch Office, 346 Broadway, New York 13, N. Y.	1
Director, Office of Naval Research Branch Office, 10th Floor, John Crerar Library Bldg., 86 E. Randolph St., Chicago 1, Illinois	1
Director, Office of Naval Research Branch Office, 1030 E. Green Street, Pasadena 1, California	1
Director, Office of Naval Research Branch Office, 1000 Geary St., San Francisco, California	1
Director, Office of Naval Research Branch Office 150 Causeway St., Boston, Massachusetts	1
Officer in Charge, Office of Naval Research, Navy No. 100, Fleet Post Office, New York, N. Y.	7
Department of Aerology, U. S. Naval Post Graduate School, Monterey, California	1
Aerology Branch, Bureau of Aeronautics (Ma-5), Navy Department, Washington 25, D. C.	1
Mechanics Division, Naval Research Laboratory, Anacostia Station, Washington 20, D. C., Attention: J. E. Dinger, Code 3820	1
Radio Division I, Code 3420, Naval Research Laboratory, Anacostia Station, Washington 20, D. C.	1
Meteorology Section, Navy Electronics Laboratory, San Diego 52, California, Attention: L. J. Anderson	1
Library, Naval Ordnance Laboratory, White Oak, Silver Spring 19, Maryland	1
Bureau of Ships, Navy Department, Washington 25, D. C., Attention: Code 851	1

Address	Copies
Bureau of Ships, Navy Department, Washington 25, D. C., Attention: Code 814	1
Bureau of Ships, Navy Department, Washington 25, D. C., Attention: Code 327	2
Chief of Naval Operations, Navy Department, Washington, 25, D. C., Attention: OP-533D	2
Oceanographic Division, U. S. Navy Hydrographic Office, Suitland, Maryland	1
Library, Naval Ordnance Test Station, Inyokern, China Lake, California	1
Project AROWA, U. S. Naval Air Station, Bldg. R-48, Norfolk, Virginia	1
The Chief, Armed Forces Special Weapons Project, P. O. Box 2610, Washington, D. C.	1
Office of the Chief Signal Officer, Engineering and Technical Service, Washington 25, D. C., Attention SIGGE-M	1
Meteorological Branch, Evans Signal Laboratory, Belmar, New Jersey	1
Office of the Quartermaster General, 2nd and T Sts., Washington 25, D. C., Attention: Environmental Protection Section	1
Office of the Chief, Chemical Corps, Research and Engineering Division, Research Branch, Army Chemical Center, Maryland	2
Commanding Officer, Air Force Cambridge Research Center, 230 Albany St., Cambridge, Massachusetts, Attention: ERHS-1	1
Headquarters, Air Weather Service, Andrews A. F. Base, Washington 20, D. C., Attention: Director Scientific Services	2
Commanding General, Air Materiel Command, Wright Field, Dayton, Ohio, Attention: MCREEO	1

Address	Copies
Commanding General, Air Force Cambridge Research Center, 230 Albany St., Cambridge, Massachusetts, Attention: CRHSL	1
Commanding General, Air Research and Development Command, P. O. Box 1395, Baltimore 3, Maryland, Attention: RDDG	1
Department of Meteorology, Massachusetts Institute of Technology, Cambridge, Massachusetts, Attention: H. G. Houghton	1
Department of Meteorology, University of Chicago, Chicago, 37, Illinois, Attention: H. R. Byers	2
Institute for Advanced Study, Princeton, New Jersey, Attention: J. von Neumann	1
Scripps Institution of Oceanography, La Jolla, California, Attention: R. Revelle	1
General Electric Research Laboratory, Schenectady, N. Y., Attention: I. Langmuir	1
St. Louis University, 3621 Olive Street, St. Louis 8, Missouri, Attention: J. B. Macelwane, S. J.	1
Department of Meteorology, University of California at Los Angeles, Los Angeles, California, Attention: M. Neiburger	1
Department of Engineering, University of California at Los Angeles, Los Angeles, California, Attention: L. M. K. Boelter	1
Department of Meteorology, Florida State University, Tallahassee, Florida, Attention: W. A. Baum	1
Woods Hole Oceanographic Institution, Woods Hole, Massachusetts, Attention: C. Iselin	1
The Johns Hopkins University, Department of Civil Engineering, Baltimore, Maryland, Attention: R. Long	1
The Lamont Geological Observatory, Torrey Cliff, Palisades, N. Y., Attention: M. Ewing	1

Address	Copies
The Johns Hopkins University, Department of Physics, Homewood Campus, Baltimore, Maryland, Attention: G. Plass	1
New Mexico Institute of Mining and Technology, Research and Development Division, Socorro, New Mexico Attention: E. Workman	1
University of Chicago, Department of Meteorology, Chicago, 37, Illinois, Attention: H. Riehl	1
Woods Hole Oceanographic Institution, Woods Hole, Massachusetts, Attention: A. Woodcock	1
General Electric Research Laboratory, Schenectady, N. Y., Attention: V. Schaefer	1
Geophysical Institute, University of Alaska, College, Alaska, Attention: C. T. Elvey	1
Blue Hill Meteorological Observatory, Harvard University, Milton 86, Massachusetts, Attention: C. Brooks	1
Department of Meteorology, University of Washington, Seattle 5, Washington, Attention: P. E. Church	1
Laboratory of Climatology, Johns Hopkins University, Seabrook, New Jersey, Attention: C. W. Thornthwaite	1
Institute of Geophysics, University of California at Los Angeles, Los Angeles, California, Attention: J. Kaplan	1
Department of Meteorology, New York University, New York, 53, New York, Attention: B. Haurwitz	1
Texas A and M, Department of Oceanography, College Station Texas, Attention: J. Freeman, Jr.	1
Massachusetts Institute of Technology, Department of Meteorology, 77 Massachusetts Avenue, Cambridge 39, Massachusetts, Attention: T. F. Malone	1
Cornell University, Department of Agronomy, Division of Meteorology. Ithaca, N. Y.	1

Address	Copies
Pennsylvania State College, School of Mineral Industries, Department of Earth Science, State College, Pennsylvania, Attention: H. Neuberger	1
Rutgers University, College of Agriculture, Department of Meteorology, New Brunswick, New Jersey	1
University of Texas, Department of Aeronautical Engineering, Austin, Texas, Attention: K. H. Jehn	1
University of Utah, Department of Meteorology, Salt Lake City, Utah, Attention: V. Hales	1
University of Wisconsin, Department of Meteorology, Madison, Wisconsin, Attention: V. Suomi	1
National Advisory Committee of Aeronautics, 1500 New Hampshire Ave., N. W., Washington 25, D. C.	2
U. S. Weather Bureau, 24th and M Sts, N. W., Washington 25, D. C., Attention: Scientific Services Division	2
Committee on Geophysics and Geography, Research and Development Board, Washington 25, D. C.	2
Air Coordinating Committee, Subcommittee on Aviation Meteorology, Room 2D889-A, The Pentagon, Washington, D. C.	1
American Meteorological Society, 3 Joy St., Boston 8, Massachusetts, Attention: The Executive Secretary	1
Research Professor of Aerological Engineering, College of Engineering, Department of Electrical Engineering University of Florida, Gainesville, Florida	1
Dr. E. G. Bowen, Chief, Division of Radiophysics, Commonwealth Scientific Industrial Research Organization, University Grounds, Chippendale, N.S.W., Australia	1
Professor Max A. Woodbury, Department of Statistics, Wharton School, University of Pennsylvania, Philadelphia 4, Pennsylvania	1

ADDITIONAL DISTRIBUTION LIST

Person or Organization	Copies
Brookhaven National Laboratory, Upton, L. I., N. Y., Attention: Meteorology Group	1
Chief, Meteorological Division, Biological Department, Chemical Corps, Camp Detrick, Frederick, Maryland	1
Dr. August Raspet, Engineering and Industrial Research Station, Mississippi State College, State College, Mississippi	2
Dr. E. W. Hewson, Diffusion Project, Round Hill, South Dartmouth, Massachusetts	1
Dr. Hunter Rouse, Director, Iowa Institute of Hydraulic Research, State University of Iowa, Iowa City, Iowa	1
Head, Department of Physics, University of New Mexico, Albuquerque, New Mexico	1
Mr. Wendell A. Mordy, Hawaiian Pineapple Research Institute, Honolulu, Hawaii	1